Recent Developments in the Ruthenium-Catalyzed Azide Alkyne Cycloaddition (RuAAC) Reaction

EurJOC
European Journal of Organic Chemistry

Review
doi.org/10.1002/ejoc.202400113

Chemistry Europe
European Chemical Societies Publishing

www.eurjoc.org

Recent Developments in the Ruthenium-Catalyzed Azide Alkyne Cycloaddition (RuAAC) Reaction

Flavia Ferrara,[a] Tamás Beke-Somfai,[b] and Nina Kann*[a]

The ruthenium-catalyzed azide-alkyne cycloaddition (RuAAC) gives access to 1,5-disubstitued triazoles in a single atom-economical step and offers advantages compared to its copper-catalyzed counterpart in that both terminal and internal alkynes can be employed. This review summarizes recent findings in this field during the last eight years, covering mechanistic investigations, synthetic developments, as well as applications in medicinal chemistry, polymer synthesis and physical organic chemistry.

1. Introduction

Defined by Sharpless et al. as the 'cream of the crop' of click reactions,[1] the azide-alkyne 1,3-dipolar cycloaddition[2] to access triazoles has become a vibrant research subject due to the wide variety of applications that this reaction has found in different fields. Over the years, many different methods for this purpose have been developed, with a significant breakthrough being metal-catalyzed azide-alkyne cycloadditions,[3] which allow tuning of the regioselectivity to obtain the desired triazole isomer. Owing to the similarity between the HOMO and the LUMO orbitals of the 1,3-dipole and the dipolarophile, the thermal Huisgen azide-alkyne cycloaddition primarily results in a mixture of 1,4- and 1,5-disubstituted triazole regioisomers (Scheme 1).[4] Regioselectivity towards the 1,4-disubstituted 1,2,3-triazole in this reaction was achieved in 2001, thanks to the discovery of the copper-catalyzed azide-alkyne cycloaddition (CuAAC), reported independently by Meldal[5] and Sharpless.[6] CuAAC quickly gained widespread recognition, especially since the mild reaction conditions and the broad substrate scope made the reaction applicable in multiple fields. Shortly after this, the need for complementary methodology to access 1,5-disubstituted 1,2,3-triazoles arose, as existing methods were inefficient and often involved stoichiometric amounts of metal.[7] This led to the discovery of the ruthenium-catalyzed azide-alkyne cycloaddition (RuAAC) by Fokin and Jia.[8] Well-known for catalyzing alkyne cyclotrimerization reactions,[9] Ru(II) complexes were investigated in the reaction of phenylacetylene

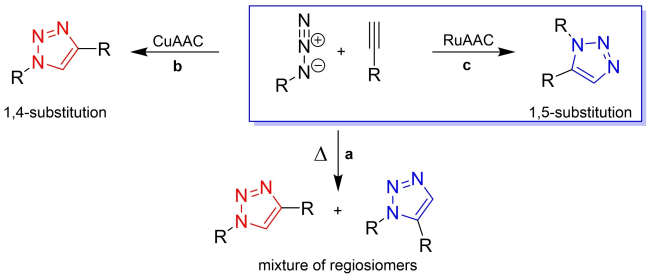

Scheme 1. Formation of 1,2,3-triazoles: (a) Huisgen thermal 1,3-dipolar cycloaddition; (b) copper-catalyzed azide alkyne cycloaddition (CuAAC); (c) ruthenium-catalyzed azide alkyne cycloaddition (RuAAC).

with benzyl azide, and were found to be capable of effectively producing 1,5-disubstituted 1,2,3-triazoles.[8] Furthermore, internal alkynes could also be utilized as substrates in RuAAC, thus expanding the substrate scope and leading to numerous applications in medicinal and organic chemistry, as well as in the development of new materials.[10] This review will primarily focus on recent advances in RuAAC from mid-2016 and onwards, following an earlier review on this topic from 2016.[11]

2. Mechanistic and Computational Studies

In a full study on the scope and mechanism of the RuAAC reaction by Lin, Jia and Fokin, the catalytic cycle shown in Figure 1 was proposed.[12] In contrast to CuAAC, internal alkynes are tolerated in the RuAAC reaction, indicating that the reaction cannot proceed via a metal acetylide.[13] The catalytically active species is proposed to be [Cp*RuCl], with the bulky pentamethylcyclopentadienyl (Cp*) ligand of importance for obtaining high regioselectivity for the 1,5-disubstituted triazole isomer. Replacing the Cl ligand with Br or I affords viable but less reactive catalysts. The reaction steps involved include ligand exchange to bind the alkyne and the azide to ruthenium (Step A, Figure 1), followed by an irreversible oxidative coupling to form a ruthenacycle (Step B), which determines the regioselectivity of the reaction.

[a] F. Ferrara, N. Kann
Department of Chemistry and Chemical Engineering
Chalmers University of Technology
SE-41296 Göteborg, Sweden
E-mail: kann@chalmers.se

[b] T. Beke-Somfai
Institute of Materials and Environmental Chemistry
Research Centre for Natural Sciences
H-1117 Budapest, Hungary

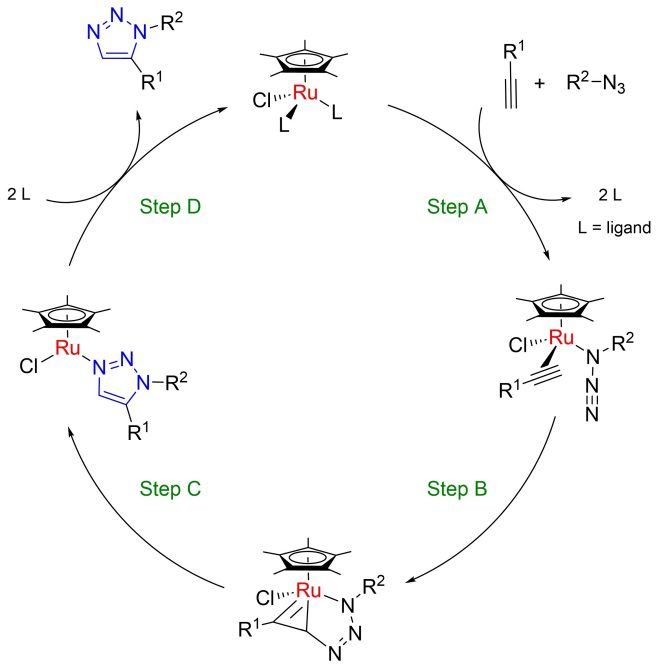

Figure 1. Proposed catalytic cycle for the RuAAC reaction. Figure adapted from Boren et al.[12]

The triazole is formed in the ensuing reductive elimination (Step C), and is then liberated from the ruthenium complex in a second ligand exchange reaction (Step D). The reductive elimination is considered to be the rate-determining step. Density-Functional Theory (DFT) calculations using the B3LYP hybrid functional were applied to further support this mechanistic proposal. Boren et al. also showed that there are a total of four possible orientations (Figure 2) that could be formed during Step A, which all have very close relative energies.[12] However, further calculations on those pathways resulted in either high energy transition states or steric clashes for the product state, which thus excluded three pathways, including those two that would have lead to 1,4-regioisomers.

Several studies have further investigated the regioselectivity of RuAAC, also testing the effect of the selected azides and alkynes on the selectivity. An underused feature of RuAAC is that it allows the use of internal alkynes, in contrast to CuAAC which is limited to terminal alkynes. In early studies, Majireck and Weinreb demonstrated that for internal alkynes, the resulting regiochemical outcome in the formation of 1,4,5-trisubstituted 1,2,3-triazoles, depended on the substitution pattern of the alkyne used (see section 3).[14] Recently, further insight on RuAAC was obtained by Benchouk and co-workers, who investigated the mechanistic aspects of the reaction with quantum chemical calculations using sugar-azides and terminal alkynes.[15] In this paper, the authors employed the B3LYP/6-31G(d) setup (with LanL2DZ for Ru and Cl) and studied how an azido derivative of ribose could interact with a terminal alkyne in presence of a ruthenium catalyst. In line with previous understanding,[12,16] their results also clearly suggested that compared to an uncatalyzed reaction, transition states with much lower energy will be present during the ruthenium-catalyzed cycloaddition. Furthermore, in terms of the regioselectivity, the initial transition state is approximately 3.48 kcal/mol lower for 1,5-disubstituted 1,2,3-triazoles compared to 1,4-disubstituted isomers, suggesting that formation of the latter is disfavored under these reaction conditions. However, it has to be noted that based on the authors' results, both directions are strongly exothermic and the two compared transition states are

Flavia Ferrara received her MSc in Organic and Biomolecular Chemistry from the Sapienza University of Rome in 2021. Soon after, she joined Prof. Nina Kann's group at Chalmers University of Technology as PhD student. Her research focuses on the development of novel triazole-based receptors for biomolecules.

Tamás Beke-Somfai received his Ph.D. in structural chemistry at Eötvös University, Budapest. He was a post-doctoral fellow, and later a guest researcher at Chalmers University of Technology, Gothenburg, Sweden. Currently he is the vice director of the Institute of Materials and Environmental Chemistry at the Research Centre for Natural Sciences (TTK), where he also leads the Biomolecular Self-Assembly research group. His research field involves theoretical and experimental investigation of natural and non-natural peptides and their assemblies, polarized light spectroscopy, and membrane-biomolecule interactions.

Nina Kann received her PhD from the Royal University of Technology KTH in Stockholm. Following a postdoc in Grenoble, and a few years as a research scientist at AstraZeneca, she is currently a professor in Organic Chemistry at Chalmers University of Technology. Her research is focused on the application of transition-metal catalyzed reactions in organic chemistry, with applications in the field of green chemistry, anticancer/antimicrobial compounds, as well as molecular sensors.

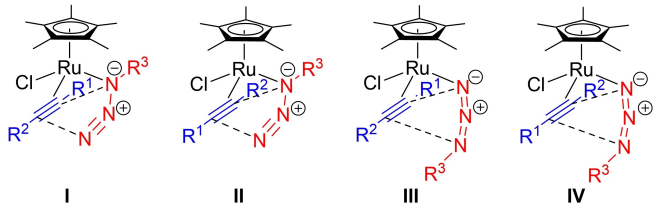

Figure 2. Activated azide/[Ru]/alkyne complexes **I–IV**.

relatively low (4.48 kcal/mol for the 1,4-isomer and 1.00 kcal/mol for the 1,5-isomer), thus in principle both regioisomers would be possible to form in the reaction. In a related study, the same authors have also performed theoretical studies at the same level of theory to predict the regioselectivity of the reaction involving benzyl azide and internal alkynes.[17] Using the four activated complexes arranged as suggested by Boren et al. (Figure 2),[12] and selecting unsymmetrical internal alkynes from those examined experimentally by Weinreb,[14] Benchouk and co-workers calculated the relative energies of the complexes, as well as their relative distribution, using the Boltzmann distribution. The resulting dominant activated complexes showed perfect agreement with the regioselectivity of the reaction observed experimentally. It is notable that the two selected sets of compounds showed opposing regioselectivity. The authors concluded that several factors contribute to this outcome, such as e.g. the formation of a nonclassical H-bond between a functional group and the Cl atom on the ruthenium center. These interactions were also confirmed by employing topological analysis by the quantum theory of atoms in molecules (QTAIM)[18] on the obtained critical points.

A similar QTAIM analysis was also performed by Hosseinnejad and Mahdavian to study the regioselectivity of Ru-catalyzed synthesis for 1,5-disubstituted 1,2,3-triazoles.[19] QTAIM obtains the topological properties of electron density and additional derived properties at bond critical points, and the related atomic interaction path reveals the charge density accumulation between the nuclei, thus indicating bond formation. Accordingly, the authors have demonstrated that the interaction between ruthenium and the acetylenic carbon, as well as the azide nitrogen, is stronger in the transition state for the 1,5-pathway than for the 1,4-path. This suggests that a larger electronic stability is present in the six-membered ruthenacycle of the former TS, rendering it more stable than the corresponding transition state (TS) for the 1,4-path.

Besides mechanistic studies, molecular simulation of 1,5-disubstituted 1,2,3-triazoles can also be applied to reach atomic level insight for e.g. enzyme binding, that may lead to the development of new drug molecules. In their recent paper, Baghersad et al. used a combined computational and experimental study, where they tested the reactivating ability of designed 1,5-disubstituted 1,2,3-triazole salicylaldoxime derivatives on paraoxon-inhibited acethylcholinesterase (AChE).[20] In this state, the latter enzyme is not active due to the neurotoxic paraoxon, which is an organophosphate used in chemical warfare. The authors employed quantum chemical, molecular docking and molecular dynamic computations to address the interaction of designed molecular structures with the paraoxon-inhibited AChE. They also calculated the reactivity and the blood brain barrier permeability of the tested 1,2,3-triazole aldoxime derivatives. The structures with the highest potential were then synthesized and tested accordingly *in vitro*. Although the reactivation effect in % of the selected compounds was lower than that of the reference drug, pralidoxime, they also showed advantageous properties that could warrant further development. Importantly, the study clearly demonstrates that by simulation advances of the recent decade, such as the advanced force field topology builder (ATB),[21] the exotic 1,5-disubstituted 1,2,3-triazoles can be implemented to biological simulations with relative ease, making application-driven computational studies feasible to perform.

3. Method Development

The regioselectivity of the RuAAC reaction, along with its catalytic activity, strongly depends on the type of ligands coordinating to ruthenium in the catalyst.[8] The most frequent applications involve the use of electron-rich pentamethyl [Cp*RuCl]-based catalysts. These 18-electron complexes, in particular [Cp*RuCl(cod)] (cod = cyclooctadiene) and [Cp*RuCl(PPh_3)$_2$], have proven to be excellent in terms of both catalytic activity and regioselectivity, consistently yielding 1,5-disubstituted 1,2,3-triazoles with high conversion of the starting materials to product. Ru-catalysts lacking the Cp* and Cl ligands generally favour the 1,4-disubstituted product or do not catalyze the reaction at all.[12,22] The optimal solvents for RuAAC reactions are typically non-protic. Commonly used options include aromatics like toluene or benzene, ethers like tetrahydrofuran (THF) or dioxane, and occasionally more polar solvents such as dimethylformamide (DMF) or dichloromethane (DCM).[11–12] Regarding the substrate scope, both aliphatic and aryl azides can be employed, and the reaction exhibits a high tolerance towards substituents on the alkyne, allowing for the use of both terminal and internal alkynes.[12] Please note that organic azides should be handled with care, as azides with a (C + O)/N ratio of less than 3 are considered to be explosive.[23]

When using internal alkynes, the presence of directing groups, usually hydrogen bond donors like propargyl amines or alcohols, plays a crucial role in governing the regioselectivity of the cycloaddition.[14] These groups form a hydrogen bond with the chloride ligand on the Ru catalyst, leading to formation of a new bond between the β-carbon and the terminal nitrogen. In cases where these hydrogen bond donor substituents are absent on the alkyne, regioselectivity is instead influenced by electronic and steric effects, with the most electronegative and least sterically hindered carbon on the alkyne ending up at the C-4 position in the final triazole product. Alkynes substituted with heteroatoms generally afford triazoles with the heteroatom located in the 5-position. Scheme 2 illustrates typical RuAAC reaction conditions for terminal and internal alkynes, as well as the impact of alkyne substituents on the regiochemical outcome.[8,12,14,24]

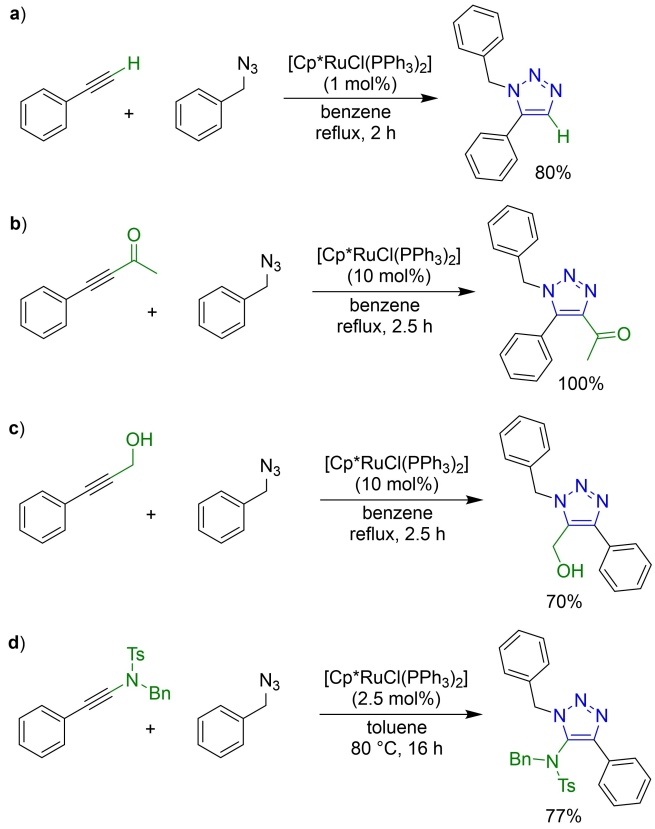

Scheme 2. RuAAC reactions of terminal alkynes (a) and internal alkynes (b-d).

Controlling the regioselectivity in RuAAC can occasionally be challenging, especially for more specialized substrates. In this context, Vaidyanathan and co-workers looked to establish a reliable procedure to enhance the regioselectivity in the synthesis of compound **1** (Scheme 3), while also facilitating easy scalability of the reaction.[25] When traditional RuAAC conditions were employed using [Cp*RuCl(PPh$_3$)$_2$] as the catalyst in refluxing dioxane, a mixture of regioisomers **1** and **2** was obtained in a 2.5 : 1 ratio (Table 1, entry 1). Notably, an improvement in regioselectivity was observed when the reaction batch became inadvertently contaminated with Pd and Cu. This led to experiments involving various additives. While the inclusion of either a Pd(0) complex or a Cu(II) salt did not yield significant differences (entries 2 and 3), the addition of CuI led to improved regioselectivity, affording a 6.2 : 1 ratio of the two regioisomers (entry 4). Unfortunately, in part due to the limited solubility of

Table 1. Additives used in the RuAAC reaction in Scheme 3.

Entry	Additive	Conversion (%)	Ratio **1**:**2**[a]
1	none	>99	2.5 : 1
2	$Pd_2(dba)_3$	>99	2.4 : 1
3	$CuSO_4$	>99	2.7 : 1
4	CuI	>99	6.2 : 1
5	$[n\text{-}Bu_4N^+]_2[Cu_2I_4]^{2-}$	>99	11 : 1

[a] Ratio determined by HPLC after TMS removal. dba = dibenzylideneacetone

CuI in the reaction medium, attempts to scale up the reaction to 1 g resulted in a reduction of the regioselectivity to 4 : 1. In the quest for a more soluble copper source, the salt $[n\text{-}Bu_4N^+]_2[Cu_2I_4]^{2-}$ proved to be the best option. This not only led to excellent regioselectivity (entry 5) but also to an enhanced reaction rate. Consequently, the reaction could be carried out at lower temperatures, achieving complete conversion within just 5 minutes at 55 °C or within 2 hours at 35 °C.

These new conditions also proved to be effective for various internal alkynes featuring alkyl and phenyl substituents, which in most cases ended up in the 4-position of the triazole. Figure 3 shows some of the products obtained when CuI was used as an additive, along with their regiochemical ratios, determined by HPLC. The results suggest that the observed regioselectivity is not dependent on the coordinating ability of the substituents on the alkyne. Additionally, both electron-withdrawing and electron-donating groups are well tolerated.

Regioselectivity for the 1,4-isomer using ruthenium catalysis has been an intriguing research topic. Previously known for promoting the formation of 1,4-disubstituted 1,2,3-triazoles,[22] Ru catalysts lacking the Cp* ligand have been a subject of consistent exploration in recent years, both in heterogeneous and homogeneous catalysis. Drawing inspiration from the previous application of a metalloprotein-inspired Ru-polymer in selective alcohol oxidation,[26] as well as the development of a Cu-based metalloprotein complex for CuAAC,[27] Pal and co-workers explored a metalloprotein-inspired Ru-polymer complex in RuAAC (Scheme 4).[28] Complex **3** displayed remarkable regioselectivity for the 1,4-isomer in cycloaddition reactions and operated under very mild conditions, i.e. using water as the solvent at ambient temperature for a mere 10 minutes. Furthermore, the low solubility of the catalyst in the reaction media facilitated recovery via filtration and the catalyst could

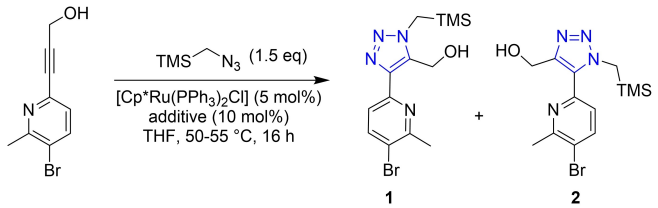

Scheme 3. The use of additives to control the regioselectivity for isomers **1** and **2** in a RuAAC reaction.

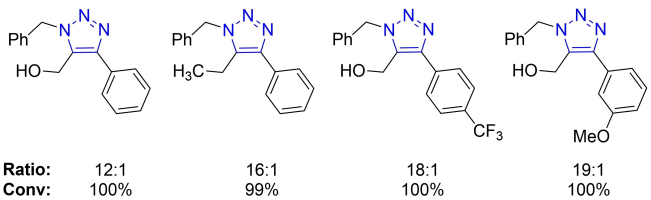

Figure 3. Regioselectivity and conversion in RuAAC reactions with 10 mol% $[n\text{-}Bu_4N^+]_2[Cu_2I_4]^{2-}$ as an additive.

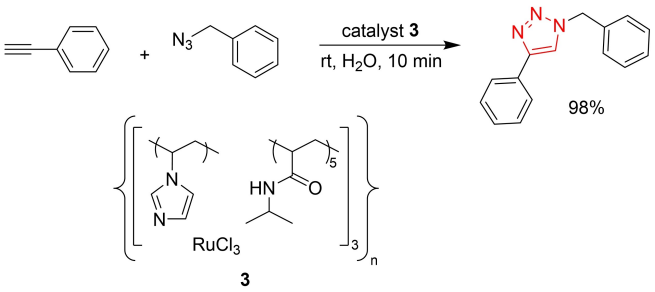

Scheme 4. RuAAC using heterogeneous polymeric metalloprotein-inspired ruthenium catalyst **3**.

be reused in six subsequent runs. These reaction conditions afforded favorable results for a wide range of substituted azides and alkynes and was easy to execute also on gram scale.

Another example of a heterogenous Ru(II) catalysis for the synthesis of 1,4-disubstituted 1,2,3-triazoles was reported by Sasson and his group.[29] Their study employed a heterogeneous Ru-catalyst, where a ligand is covalently linked to SBA-15, an easy functionalizable mesopourous material known for its hydrothermal stability, thick pore walls and large pore size. The free hydroxyl groups on SBA-15 can be readily functionalized with an azido linker, which is subsequently clicked together with a propargylamine. This resulting ligand is then mixed with a solution of $[RuCl_2(PPh_3)_3]$ to yield catalyst **4** (Scheme 5). This Ru complex served as an excellent catalyst in a multicomponent cycloaddition reaction involving an alkyne, sodium azide and a benzyl bromide. The optimal reaction conditions were found by employing 0.5 mol% of the heterogenous catalyst at 90 °C in water as a solvent. The reaction worked for a broad scope of functionalized arylacetylenes, with yields varying from 70 to 92% (see Scheme 5 for some examples).

Arafa et al. explored the Ru-catalyzed formation of 1,4-disubstituted 1,2,3-triazoles using ultrasonic irradiation.[30] Aiming at solving most of the common issues for RuAAC, they developed a protocol with mild reaction conditions, replacing thermal activation with ultrasonic irradiation as the energy source. This innovation allowed the reaction to be conducted at room temperature in water as the solvent. Their investigation encompassed various organic azides and functionalized alkynes, employing freshly prepared catalyst **5** (Figure 4). Remarkably, yields for RuAAC exceeded 99% in all cases, using reaction times of up to 10 minutes. Additionally, when the procedure was applied towards a symmetrical internal alkyne (dimethyl acetylenedicarboxylate) in reactions with phenyl azide and benzyl azide respectively, the obtained yield was 99% for both reactions.

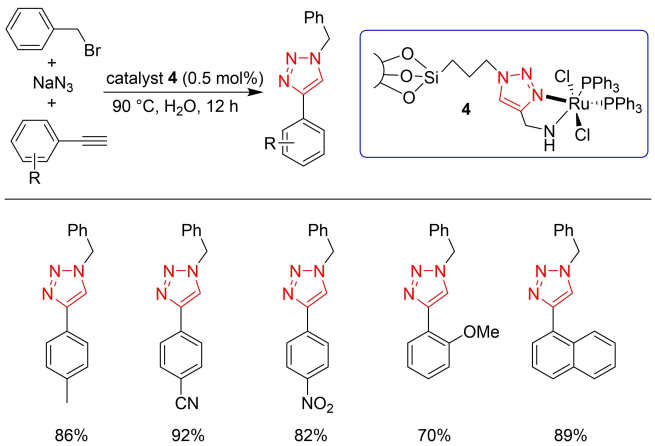

Scheme 5. Heterogeneous RuAAC catalysis using complex **4**.

Furthermore, complex **5**, under ultrasonic irradiation, also proved able to catalyze a multicomponent azide alkyne cycloaddition, involving sodium azide, benzyl halides and alkynes, affording almost quantitative yields of the desired products (Scheme 6).

In addition to the regioselectivity, the chemoselectivity of the RuAAC reaction has also been explored, focusing both on the azide and on the alkyne. In particular, Ferreira and co-workers developed a new method for the synthesis of 1,3-diynes and tested them in RuAAC, in order to explore both the chemoselectivity and the regioselectivity.[31] They showed that of the two alkyne functionalities present in compound **6** (Scheme 7), only the alkyne proximal to the alcohol reacted with benzyl azide under RuAAC conditions, while the alkyne distal to the hydroxyl group remained intact, yielding a 5:1 regioisomeric mixture of compounds **7** and **8**. Hypothetically, hydrogen bond formation between the hydroxyl functionality and the Cl ligand on the catalyst not only directs the regioselectivity of the reaction, but also imparts the chemoselectivity, making the propargylic position the most reactive one.

Looking at discriminating between different type of azides, Hosoya and colleagues reported two different studies concerning the functionalization of a triazide and a tetraazide compound. In the first investigation, the selectivity towards

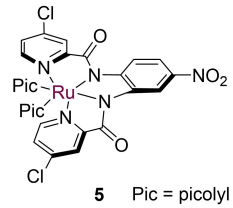

Figure 4. Ruthenium-complex **5** for use in ultrasound-mediated RuAAC.

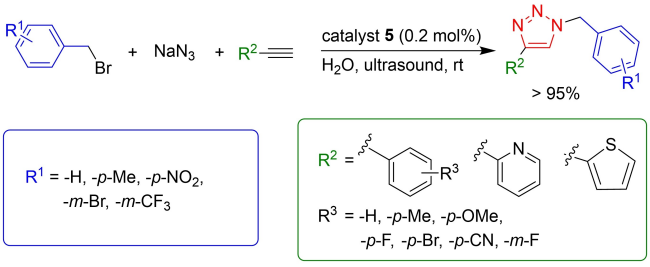

Scheme 6. Multicomponent ultrasound-mediated RuAAC with catalyst **5**, affording 1,4-disubstituted triazole isomers.

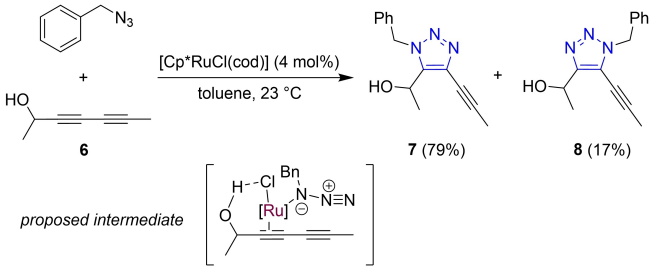

Scheme 7. Regio- and chemoselectivity in the RuAAC reaction of 1,3-diyne **6** with benzyl azide (cod = cyclooctadiene).

three different types of azides was explored, including 1) a sterically hindered aromatic azide (2,5-isopropylphenyl azide), 2) a standard aromatic azide (phenyl azide) and 3) an aliphatic azide (benzyl azide).[32] By setting competitive experiments in which they used an equimolar mixture of the azides in different cycloaddition conditions, they found the reactions catalyzed by [Cp*RuCl(PPh$_3$)$_2$] to be highly selective for the benzyl azide and regioselective in terms of forming the 1,5-disubstituted 1,2,3-triazole. After developing conditions to functionalize the other two azides via a strain promoted click reaction and a base catalyzed 1,3-diketone cycloaddition reaction, they tested these three reactions in sequence on tri-azide **9**, achieving the desired selectivity and a 79% yield of tris-triazole **10** over three steps (Scheme 8).

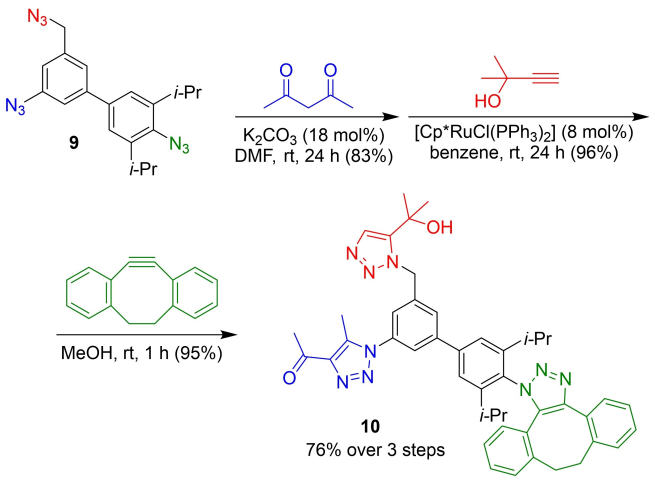

Scheme 8. Consecutive triazole formation to form **10** using three different reactions.

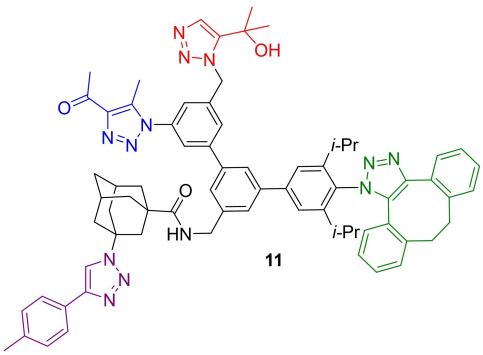

Figure 5. A tetra-triazole (**11**) formed via four consecutive triazole-forming reactions.

The same research group has also used this method to tackle azido-type selective functionalization of a tetraazide, where RuAAC was again employed for the selective functionalization of the benzyl azide moiety to form compound **11** (Figure 5).[33]

Chemoselectivity in ruthenium-catalyzed azide thioalkyne reactions (RuAtAC) was also successfully achieved by Mascareñas and co-workers, who found a way to carry out the reaction between azides and thioalkynes in water using [Cp*RuCl(cod)] as the catalyst.[34] The reaction conditions were applicable towards a broad range of azides and thioalkynes, affording 4-alkylthio-substituted triazoles **12** in excellent yields with high regioselectivity (Scheme 9). When a normal internal alkyne without a thio-substituent was used (**13**, Scheme 10), the reaction was somewhat slower and afforded a 5:1 mixture of regioisomers of triazole **14**. In a competitive cycloaddition experiment involving **13** and a thioalkyne, the only triazole formed was the one derived from the thioalkyne, demonstrating the higher reactivity of the thioalkyne under these conditions.

Complete chemoselectivity in these types of reactions was achieved some years later by the same group.[35] In their quest to develop a method that was effective under dilute micromolar conditions, they identified cationic Ru(II) complexes, such as

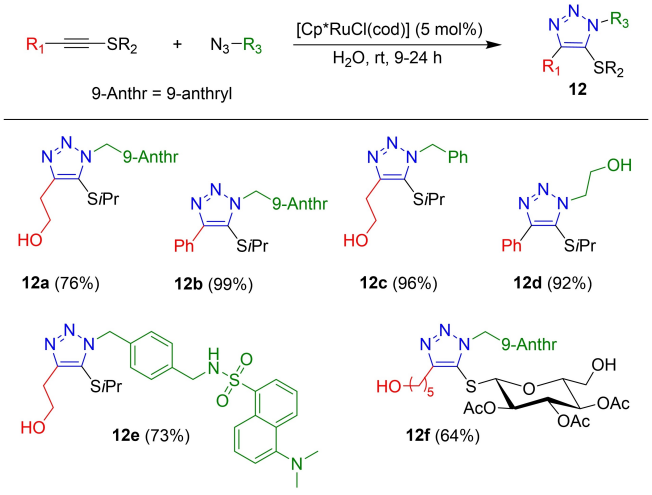

Scheme 9. Ruthenium-catalyzed azide thioalkyne (RuAtAC) reactions in water, affording 4-thiotriazoles **12**.

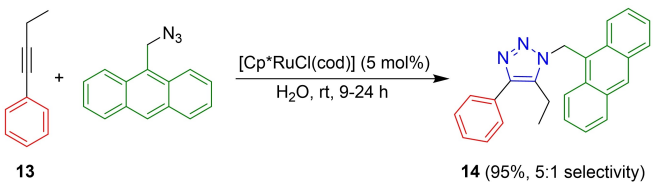

Scheme 10. RuAAC in water using internal alkyne **13**.

$[Cp^*Ru(MeCN)_3]PF_6$, as exceptional candidates for this purpose. These complexes displayed a high activity for the RuAtAC reaction in aqueous environments, which is likely due to active Ru(II) aquo or oxo derivatives that favour the 1,3-cycloaddition pathway. In addition to promoting a regioselective reaction for a broad range of substrates, these ruthenium catalysts demonstrated a lack of reactivity when tested in reactions involving alkynes lacking the thioether functionality. Building upon this observed chemoselectivity, Mascareñas and co-workers explored the orthogonality between CuAAC and RuAtAC by conducting test conditions with azide **15** and alkynes **16a** and **16b** (Scheme 11).[35] After verifying that $[Cp^*Ru(MeCN)_3]PF_6$ as the catalyst yielded compound **17a** exclusively (Table 2, entry 1), while $CuSO_4 \bullet 5H_2O$, in the presence of sodium ascorbate selectively afforded compound **17b** (entry 2), they tried these two catalysts in combination. Sequential addition of the Cu-catalyst, followed by the Ru-catalyst and a second equivalent of azide after 2 hours, afforded high yields of both products **17a** and **17b** (entry 3) and similar results were found when reversing the order of addition of the catalysts (entry 4). When Cu and Ru were both present from the outset, using one equivalent of azide, the reaction resulted in an equal mixture of compounds **17a** and **17b** (entry 5). The results demonstrate that these catalysts are highly chemoselective but also mutually orthogonal, indicating that they could potentially be used for selective dual tagging of biomolecules. This chemoselectivity and orthogonality arises due to the fact that the $[Cp^*Ru(MeCN)_3]PF_6$ catalyst is selective for thio-substituted alkynes and does not afford any triazole in reactions with normal alkynes, while the CuAAC reaction is instead limited to terminal alkynes as substrates, due to the formation of an intermediate copper-acetylenide species.[36]

A strategy to access 1,4,5-trisubstituted 1,2,3-triazoles having a thiocyanate group in the 5-position has been developed by Song and Zheng with colleagues.[37] Thiocyanates show high bioactivity in many natural products, and are also good leaving groups. In addition, triazolyl organosulfur compounds are widely used in agriculture and as chiral ligands for asymmetric catalysis. The optimized reaction conditions were tried on thiocyano-alkynes and azides with different substitution patterns (see Scheme 12 for selected products). The yield obtained was high for many of the substrates, both internal alkynes with various substituent on the aromatic ring (**18a**–**b**) and different types of alkyl azides (**18c**–**d**), including a secondary azide (**18e**). Yields were lower, however, when the other substituent on the alkyne was an aromatic heterocycle (**18f**–**g**) or when an aryl azide was used (**18h**).

Encouraged by the successful outcome of this procedure, Song and Zheng with colleagues also explored a RuAAC/nucleophilic substitution cascade reaction, to produce 5-sulfur-1,2,3,–triazoles **19** (Scheme 13).[37] The best results were obtained when using -CN as a leaving group for the sulfur substituent on the internal alkyne in combination with Grignard reagents as nucleophiles. The reaction worked well with primary, secondary and especially aryl Grignard reagents, with

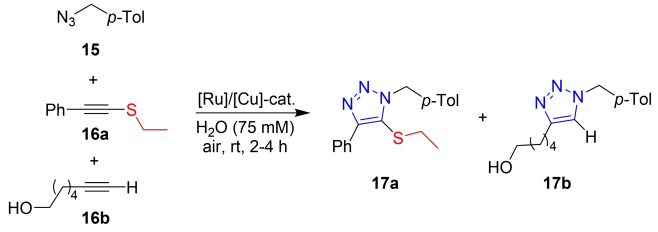

Scheme 11. Orthogonality test between RuAtAC and CuAAC reactions. Conditions, see Table 2.

Table 2. Catalysts and conditions used in an orthogonality test between RuAtAC and CuAAC reactions, see Scheme 11.[a]

Entry	Catalyst[b]	Yield **17a** (%)[c]	Yield **17b** (%)[c]
1	[Ru] (2 h)	79	0
2	[Cu] (2 h)	0	78
3	[Cu] (2 h), then [Ru] (2 h)[d]	79	78
4	[Ru] (2 h), then [Cu] (2 h)[d]	78	95
5	[Ru] and [Cu] (2 h)	44	50

[a] Equimolar amounts of **15**/**16a**/**16b** used. [b] [Cu]: $CuSO_4 \cdot 5H_2O$ (5 mol%), NaAsc (10 mol%); [Ru]: $[Cp^*Ru(MeCN)_3]PF_6$ (5 mol%). [c] Yield determined by ^1H NMR. [d] After 2 h, a second equivalent of azide **15** was added, followed by the second catalyst.

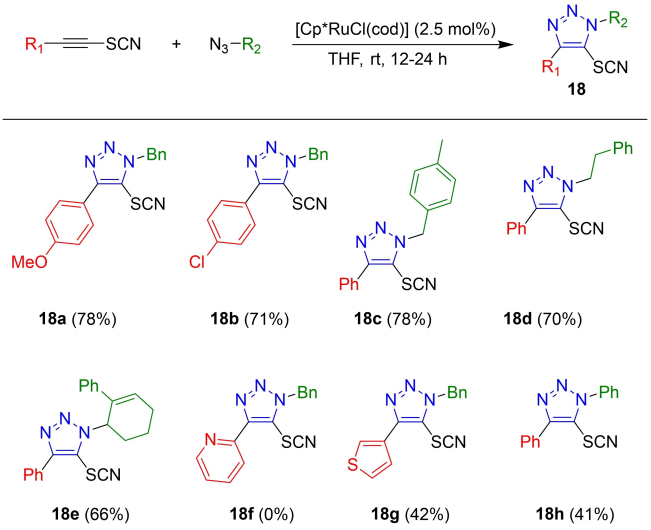

Scheme 12. Fully substituted 5-thiocyanato-1,2,3-triazoles **18** prepared via RuAAC.

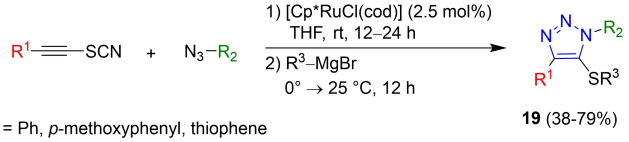

R^1 = Ph, *p*-methoxyphenyl, thiophene

R^2 = Bn, $-CH_2CH_2Ph$

R_3 = Pr, *i*-Pr, Ph, Bn, *p*-Cl-phenyl, cyclopentane, cyclopropane

Scheme 13. Cascade RuAAC/nucleophilic substitution reaction for the synthesis of fully substituted 5-sulfur-1,2,3-triazoles **19**.

benzyl and phenylethyl azide, and with some different types of 4-substituted 5-thiocyano internal alkynes

Goswami and colleagues have also investigating the synthesis of 2-triazolyl thio/selenopyridines.[38] They initially explored the substrate scope of the reaction between 1-alkynyl thio/seleno cyanates with aryl and alkyl azides, obtaining good yields for the synthesis of both thio- and seleno- substituted triazoles. Reactions with SeCN-substituted alkyne proceeded regioselectively, only affording the 5-SeCN-substituted triazole. However, for the azide thiocyano-alkyne cycloaddition, regioisomers were obtained in ratios ranging from 7.6:1 to 11:1, with the major isomer being the 5-SCN triazole. With this methodology in place, the possibility of forming 2-triazolyl thio- and seleno-pyridines **20** and **21** (Scheme 14), by reacting the previously synthesized thio/seleno substituted triazoles with 1,6-diynes via a [2+2+2] cycloaddition, was also explored. The high yields obtained, and the fact that the same catalyst can be used for both cycloadditions, encouraged the group to develop a one-pot [3+2]/[2+2+2] cycloaddition procedure. After optimizing the reaction conditions, the substrate scope was explored, including various symmetrical 1,6-diynes and 1-alkynyl thiocyano/selenocyanates in the presence of different azides. While the other regioisomer was observed in a few cases, moderate to good yields and high regioselectivity was obtained for most products.

To conclude with new methods developed for RuAAC, it is important also to mention solid phase versions of this reaction.

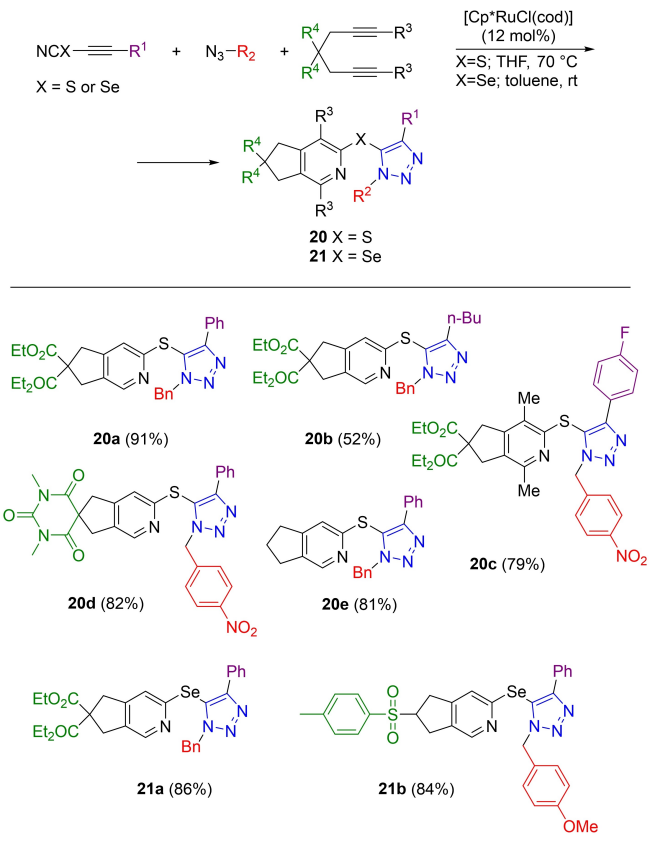

Scheme 14. One-pot Ru-catalyzed [3+2]/[2+2+2]-cycloaddition to form 2-triazolyl thio- and selenopyridines **20** and **21** (selected examples).

Secondary azides are usually less reactive than primary ones, which negatively impacts the reaction rate of the cycloaddition. Desiring to broaden the scope of RuAAC by using secondary peptide-azides, Blixt and co-workers developed a catalytic system using [Cp*RuCl(cod)] in conjunction with polymer-supported azidopeptides, affording triazolyl peptides **22** in good yields (Scheme 15).[39] The reaction afforded almost quantitative conversion of both internal and terminal alkynes, with few exceptions.

4. Medicinal and Biological Applications

Both 1,4- and 1,5-disubstituted 1,2,3-triazoles have found widespread applications in the area of medicinal chemistry and for biological purposes, both as a means of connection or deriviatizing molecules, but also to exploit the polar and hydrogen bonding properties of the triazoles themselves.[11,40] In this chapter we look at the various uses of 1,5-disubstituted 1,2,3-triazoles in this context, including also reports on 1,4,5-trisubstituted triazoles

4.1. Peptidomimetics and Foldamers

The most common usage of RuAAC in medicinal chemistry is in the area of peptidomimetics, and there are several situations where a triazole can be useful in this context. A triazole as part of a peptide sequence can act as a peptide bond isostere.[41] RuAAC can also be used to effect ring-closure of a cyclic

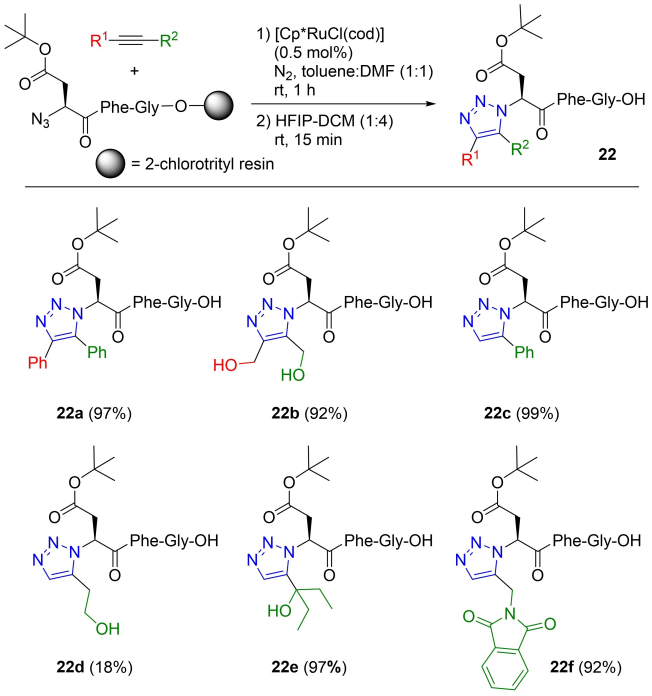

Scheme 15. Solid phase RuAAC with polymer supported secondary azides to form triazolyl peptides **22** (selected examples). Conversion determined by HPLC before purification.

peptide, and 1,5-disubstituted 1,2,3-triazoles have been investigated as mimics for disulfide bonds. In addition, RuAAC has been exploited in foldamer synthesis, as well as for derivatizing the side chains of individual amino acids in a peptide.

Triazoles can act as isosteres for peptide bonds, where the 1,4-disubstituted 1,2,3-triazole mimics a *trans*-amide bond, while a triazole with a 1,5-disubstitution pattern instead resembles a *cis*-amide bond in terms of the distance between adjacent α-carbon atoms.[41] Filippov and colleagues exploited this feature in the synthesis of histidine isosteres, in order to probe the involvement of histidine residues in ADP-ribosylation processes by using 1,4- and 1,5-disubstituted 1,2,3-triazoles as mimics for N(τ)- and N(π)-ribosylated histidine.[42] Building block **23**, as well as a stereoisomer thereof, were prepared from the corresponding azide and alkyne using [Cp*RuCl(cod)] as the catalyst under microwave conditions (Scheme 16). Using the alkyne in excess was found to be important in order to attain an acceptable yield. The corresponding 1,4-isomers were prepared via CuAAC and the regioselectivity of all derivatives was verified using 2D NMR. The building blocks were then incorporated into peptide sequences using Fmoc-based solid phase peptide synthesis. The hydrolytic stability of the peptides in the presence of (ADP-ribosyl)hydrolase was then evaluated, showing that the 1,5-isomers were more labile than their 1,4-counterparts, with **23** displaying the highest hydrolysis rate, indicating that α-N(π)-His could be the natural isomer. Further studies are needed, however, to clarify if this hydrolysis is of biological relevance or caused by the inherent lability of the 1,5-triazole building block **23**.

Mucha and colleagues have reported the synthesis of 5-bromo-substituted-1,4,5-trisubstituted amino acid **24** in high yield using [Cp*RuCl(PPh$_3$)$_2$] (Scheme 17).[43] Following ester hydrolysis, the cytotoxicity of the resulting carboxylic acid was evaluated against two human cell lines (immortal human keratinocyte and skin fibroblast), with no effect on cell viability detected, indicating that this amino acid building block is well tolerated by human cells. Zhao and Burke Jr. attempted to modify an alkyne-labeled peptide on solid phase via RuAAC with [Cp*RuCl(PPh$_3$)$_2$] as the catalyst, aiming to prepare polo-like kinase inhibitors.[44] Somewhat surprisingly, a diagnostic ^{13}C NMR signal for the resulting triazole was found to be identical to that of the corresponding derivative prepared via CuAAC, indicating that the 1,4-disubstituted triazole isomer was formed instead. The authors do not provide any explanation for this anomalous behavior.

In addition to incorporating triazole-containing amino acids as single unit replacements in a peptide chain, another approach towards peptidomimetics is to assemble the entire peptide chain using triazole building blocks. Angelo and Agora reported such peptidotriazolamers deriving from 1,4-disubstituted 1,2,3-triazoles in 2005.[45] Our research group has in turn prepared peptidotriazolamers from 1,5-disubstituted triazole units and studied their structural and conformational properties using 2D NOESY NMR and quantum mechanics.[46] In a more recent investigation, we instead performed a systematic synthetic and quantum chemical study of the conformational properties of all eight possible chiral derivatives of a triazole building block, prepared via RuAAC, focusing on the effect of placing a chiral substituent on either or both sides of a triazole amino acid (Figure 6).[47] [Cp*RuCl(cod)] was found to be the best catalyst for preparing the chiral triazole amino acids **25**, as other Ru-catalysts required a higher reaction temperature, resulting in some loss of enantioselectivity. The folding properties of peptidotriazolamer (*S*,*S*,*S*)-**26**, constructed using three units of **25 b**, was also investigated.

Peptidotriazolamers can also be prepared using different chiral building blocks instead of forming a homooligomer. As mentioned earlier, triazoles with a 1,4- and 1,5-substitution pattern can act as mimics for *trans*- and *cis*-peptide bonds,[41] although the 1,5-disubstituted triazole provides a better fit for the *cis*-configuration in this respect. Sewald and co-workers

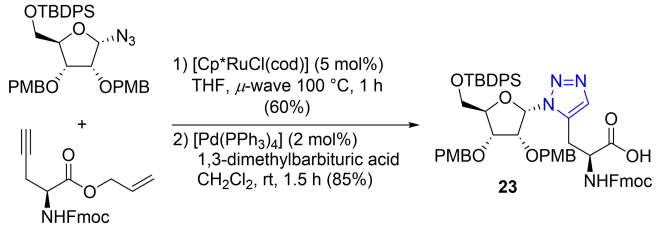

Scheme 16. 1,5-1,2,3-triazole **23** as a mimic for ADP-ribosylated histidine (PMB = *p*-methoxybenzyl; TBDPS = *tert*-butyldiphenylsilyl; Fmoc = fluorenylmethoxycarbonyl).

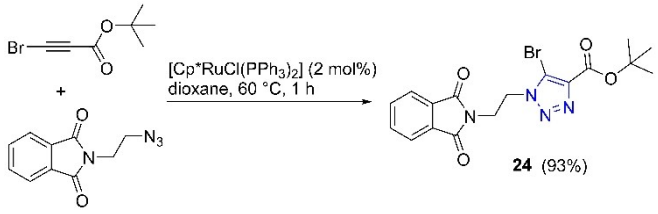

Scheme 17. Synthesis of 5-bromo-1,2,3-triazole **24** as an amino acid mimic.

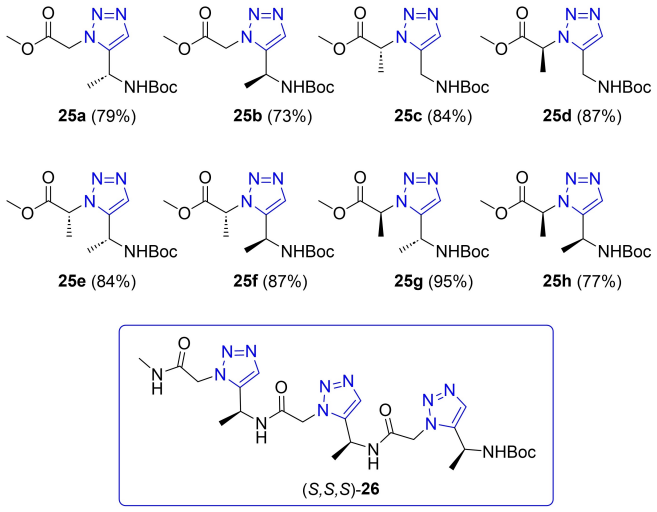

Figure 6. Eight possible possible chiral triazole amino acid derivatives (**25**) prepared via RuAAC and a trimeric peptidotriazolamer (**26**) assembled from one of these building blocks (Boc = *tert*-butyloxycarbonyl).

exploited this feature in the synthesis of peptidotriazolamers **27** and **28** (Figure 7).[48] While the chiral azide precursors were relatively easy to assemble from commercial amino acid benzyl ester salts in good yields, synthesis of the chiral alkyne starting materials was substantially more challenging due to facile racemization of the chiral centre. Using a *tert*-butylsulfinamide-based chiral auxiliary reported by Ellman,[49] and modifying the work-up procedure in order to avoid chromatographic purification, the desired alkynes could be prepared in enantiomerically pure form. Microwave-assisted RuAAC, using 3–5 mol% [Cp*RuCl(cod)] as the catalyst in THF, afforded a set of six different chiral triazoles in excellent yields, ready to be assembled into trimeric peptidotriazolamers. *sym*-Collidine was used to liberate the amine from the corresponding HCl-salt after Boc deprotection. HOAt was subsequently applied as the coupling agent, producing peptidotriazolamers **27** and **28** in high yields.

RuAAC provides a convenient means for fusing a macrocyclic peptide and this feature has been explored by Liskamp and co-workers in the synthesis of mimics of the antibiotic vancomycin (Figure 8).[50]

In earlier work, the group targeted CDE-ring mimics,[51] while in a more recent study, bicyclic mimics of the ABC-ring were instead prepared.[52] Precursor **29** was initially cyclized to **30** using ring-closing metathesis in order to form the first of the two rings (Scheme 18). Coupling to the alkyne-containing phenylglycine building block **31** then set the stage for forming the second ring via RuAAC. Treatment with $[Cp^*RuCl]_4$ under microwave conditions afforded the desired triazole in 22% yield. Boc-deprotection, followed by separation of the *E/Z* isomers using preparative HPLC, afforded mimetics **32a** and **32b**. An alternative strategy, where RuAAC was performed before ring-closing metathesis, was not successful.

The same group also investigated a double-cyclization strategy to access vancomycin mimic **33** (Scheme 19), which was prepared from precursor **34** using 20 mol% $[Cp^*RuCl]_4$ as the catalyst.[53] Mimic **33** showed a promising minimum inhibitory concentration (MIC) value of 37.5 μg/mL, in comparison to 2 μg/mL for vancomycin itself.

Several groups have recently explored 1,5-disubstituted 1,2,3-triazoles as mimics for disulfide bonds. Disulfide bonds are formed between two cysteine units and are important for stabilizing structural motifs in peptides and other bioactive molecules, in this way affecting their bioactivity.[54] However, the disulfide bond can also be unstable under reducing conditions and in the presence of certain enzymes. In addition, scrambling of disulfides can take place if several cysteine units are present, producing isomeric structures that are incorrectly folded, which may affect the bioactivity. Much research has thus been devoted to finding more stable alternatives for this linkage.[54] Jamieson and co-workers investigated if the 1,5-disubstituted 1,2,3-triazole could replace a disulfide bond in a

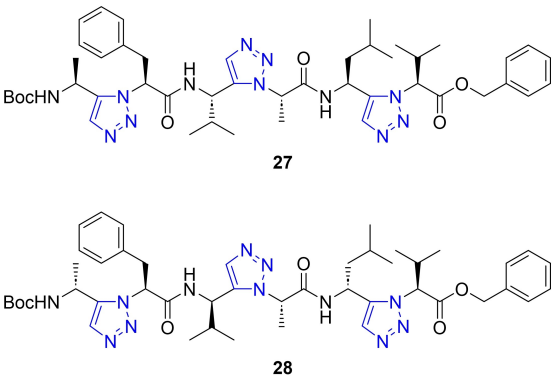

Figure 7. Chiral peptidotriazolamers **27** and **28** with 1,5-disubstituted 1,2,3-triazoles as a mimics for *cis*-peptide bonds.

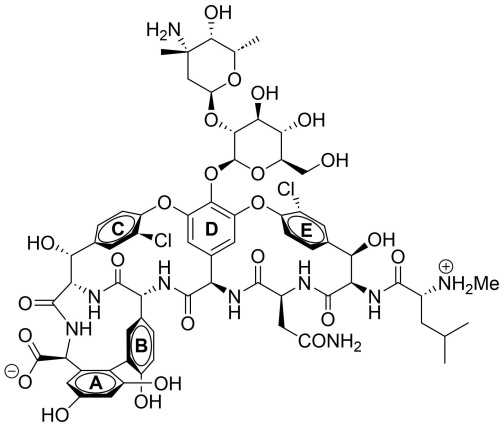

Figure 8. The antibiotic vancomycin.

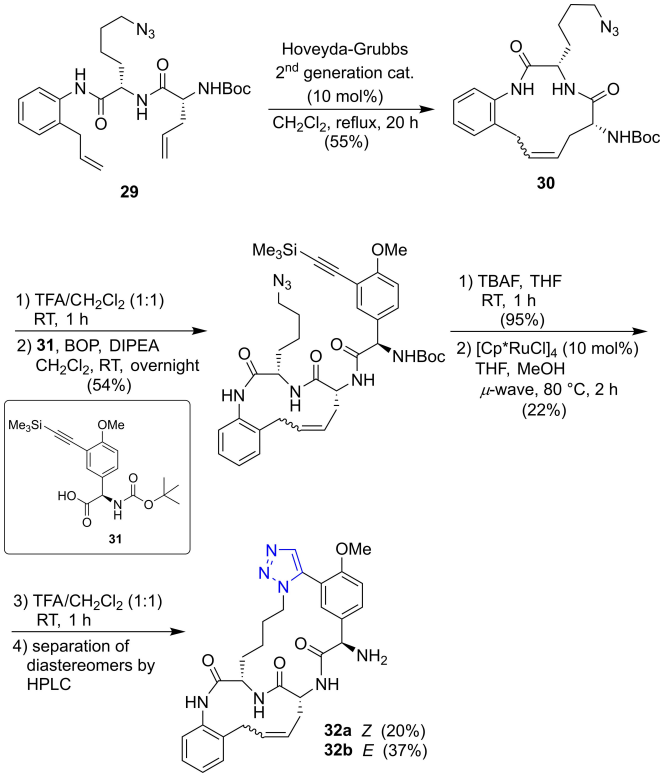

Scheme 18. Mimic **32** of the vancomycin ABC-ring system (Boc = *tert*-butyloxycarbonyl).

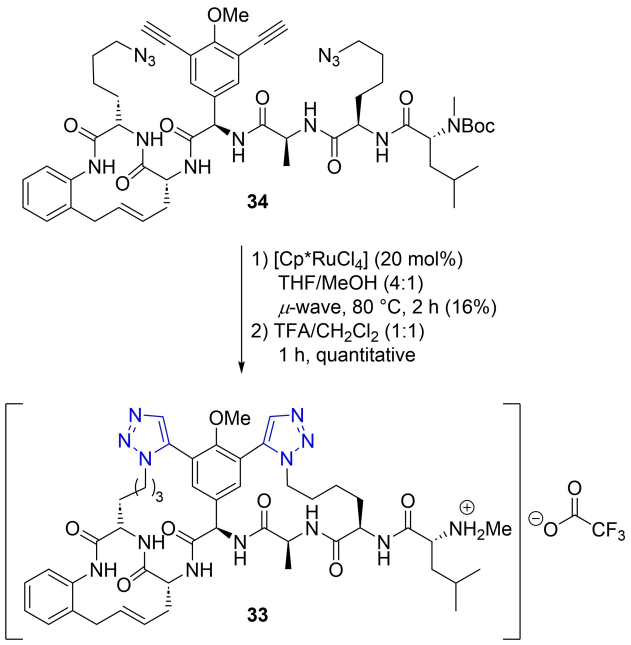

Scheme 19. A double-RuAAC strategy towards a mimic of the antibiotic vancomycin.

urotensin-II mimetic.[55] The urotensin-II receptor (UTR) is a subclass of G-Protein Coupled Receptors (GPCRs), which are transmembrane proteins important for cell signalling and for retaining a normal physiological function. UTR binds pseudo-irreversibly to the cyclic peptide urotensin-II (U-II), which contains a disulfide bond. Studies of analogues of U-II have shown that an octapeptide is required for biological activity and a Trp-Lys-Tyr fragment was identified as the pharmacophore.[56] It was postulated that disulfide bond shuffling could lie behind the irreversibility, with a new covalent disulfide bond being formed between U-II and a cysteine unit in the receptor. To investigate this, the disulfide was replaced with a more robust triazole linkage. Peptidomimetic **35** (Figure 9) was prepared using microwave-assisted solid phase peptide synthesis, where macrocyclization via RuAAC was carried out on solid support using [Cp*RuCl(cod)] as the catalyst. The corresponding 1,4-disubstituted triazole analogues was also prepared for comparison. Both peptidomimetics showed high affinity to UTR in *in vitro* binding studies, and were also shown to bind reversibly, using wash-on wash-off protocols. This indicates that the disulfide bond is most likely responsible for the irreversible behaviour of urotensin-II itself.

The same research group has also investigated α-conotoxin GI triazole peptidomimetics, using a triazole as a surrogate for disulfide bonds. α-Conotoxin GI has been isolated from the venom of a marine predatory snail, *Conus geographus*,[57] and is under investigation as a potential therapeutic for type 2 diabetes and hypertension.[58] The linear GI peptide contains 13 amino acids, with cysteine units in positions 2, 3, 7 and 13, providing several possibilities for disulfide bond formation under oxidative conditions. Jamieson and colleagues investigated two different mimics for such compounds by replacing

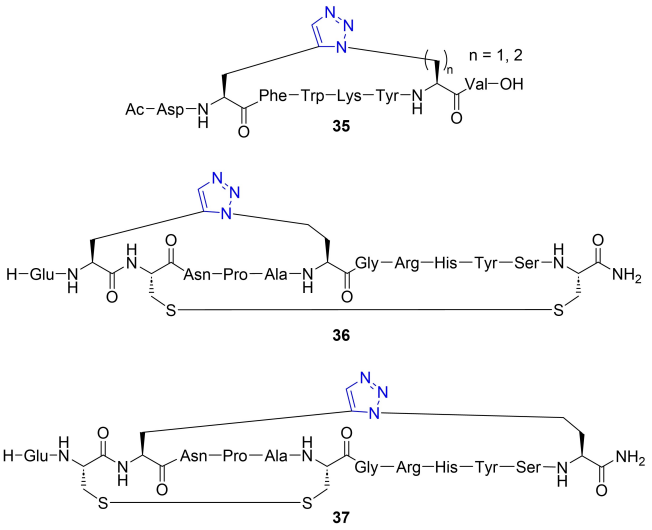

Figure 9. Triazoles as disulfide replacements in urotensin-II mimics (**35**) and α-conotoxin GI mimics (**36**-**37**).

[Cys2-Cys7] (**36**) as well as [Cys3-Cys13] (**37**) with a 1,5-disubstituted triazole (Figure 9). Mimetic **37** showed biological activity comparable to α-conotoxin GI and was also more stable in plasma, while mimetic **36** was inactive. The solution structure of **37** also showed good overlap with the NMR and crystal structures of the native α-conotoxin GI peptide, showing that the triazole unit is an effective replacement for a disulfide bond in this context.

Triazoles have also been used as disulfide bond mimics in chimeric melanocortin peptides by Haskell-Luevano and colleagues.[59] Melanocortin receptors are important for a number of physiological functions, such as pigmentation, inflammation and exocrine gland function. This group targeted a chimeric AGRP (agouti-related protein) melanocortin peptide, where 1,5-disubstituted 1,2,3-triazoles were introduced to replace a disulfide bond in mimics **38** and **39** (Figure 10). Peptidomimetic **38** was found to have equipotent activity in comparison to the natural peptide, while **39** showed reduced potency. The triazoles were prepared with the peptidomimetic precursor tethered to a polystyrene support, using 20 mol%

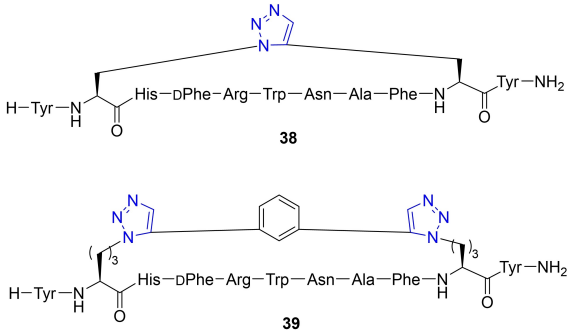

Figure 10. Triazoles **38** and **39** as disulfide bond mimics in melanocortin peptides.

[Cp*RuCl(cod)] as the catalyst, under microwave heating in dimethylformamide at 60 °C for 3 hours.

Durek and Craik used triazoles as disulfide bond mimics in cyclic protease inhibitors, based on the sunflower trypsin inhibitor-1 (SFTI-1).[60] The precursor peptides were assembled using solid phase peptide synthesis, incorporating commercially available azide and alkyne precursors, and subsequently backbone cyclized after cleavage, to bring the two reactive moieties closer to each other. Conditions for RuAAC involved the use of 50 mol% [Cp*RuCl(cod)] in anhydrous DMF at 80 °C for 18 hours, affording six different 1,5-disubstituted 1,2,3-triazoles (**40**, Figure 11). ^{1}H NMR analysis and x-ray crystallography showed that the triazole derivatives adopted similar conformations to the natural peptide and were also highly resistant to degradation in human serum, indicating that the 1,5-disubstituted triazole unit is an excellent replacement for a disulfide bond in these types of peptidomimetics.

4.2. DNA Mimics

There are several options for introducing a triazole ring into a DNA mimic, i.e. replacing a phosphodiester, a sugar moiety or a nucleobase, or alternatively placing a triazole in the terminal position. Brown and his group have earlier studied the effect of triazoles as components in DNA mimics, initially focusing on 1,4-disubstituted 1,2,3-triazoles,[61] but later also including 1,5-disubstituted triazoles in such structures.[62] Incorporation of triazoles into oligonucleotides has been shown to improve their stability towards nuclease degradation and reduce their overall anionic charge. In two recent studies, the Brown group incorporated 1,5-disubstituted 1,2,3-triazoles into the backbone of oligonucleotides using RuAAC.[63] In the first of these studies, triazole **41** was prepared in excellent yield from alkyne **42** and azide **43**, using [Cp*RuCl(PPh$_3$)$_2$] as the catalyst (Scheme 20).[63a] Phosphitylation of **41**, using **44** as the reagent, afforded phosphoramidite **45**, ready for introduction into an oligonucleotide. The distance between the adjacent methylene carbons on a 1,5-disubstituted triazole (**45**) is shorter than that for a 1,4-disubstituted isomer (**46**). In addition, the 1,5-isomer provides a 6-bond spacer between the sugar units, in contrast to the 7-bond spacer of the 1,4-isomer. Melting temperatures of duplexes formed from oligonucleotides containing either **45** or **46** and DNA were found to be slightly reduced (T_m = 59.0 °C or 54.5 °C, respectively) in comparison to the unmodified DNA control (T_m = 61.9 °C). A higher T_m corresponds to a stronger duplex, so this indicates that while both triazole-DNA derivatives are destabilizing compared to the control, the oligonucleotide containing **45** is a better mimic for DNA than the derivative from **46**, with only a slight deviation in the melting temperature.

A similar trend was seen when comparing duplexes with complementary RNA, where **45** again performed better in terms of stability. In this case, improved results were obtained for a 1,4-isomer mimic with a 6-bond spacer (i.e. one bond shorter than for **46**), indicating that a 6-bond linkage is the optimum spacer length for a triazole-containing DNA backbone mimic.

In a later study, the DNA backbone mimics **47** and **48** were prepared (Figure 12). These compounds are analogues of triazoles **45** and **46** in Scheme 20, but with a different sequence of atoms in the spacer.[63b] The stability of oligonucleotides containing a 6-bond spacer was here confirmed, with oligonucleotides containing **47** forming more stable DNA and RNA duplexes compared to oligonucleotides with **48** incorporated. In addition, the DNA polymerase replication properties of oligonucleotides containing each of the four spacers **45**, **46**, **47** and **48**, was investigated. The oligonucleotide prepared from **47** showed both higher read-through accuracy and superior replication kinetics in comparison to the other triazole-containing oligonucleotides.

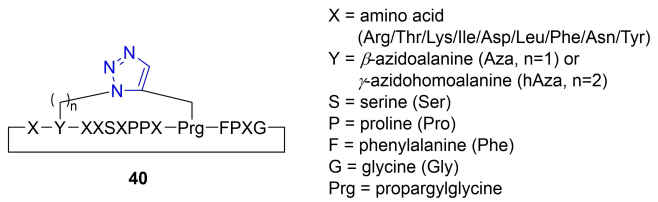

Figure 11. Triazoles as disulfide bond mimics in cyclic protease inhibitors **40** based on the sunflower trypsin inhibitor-1 (SFTI-1).

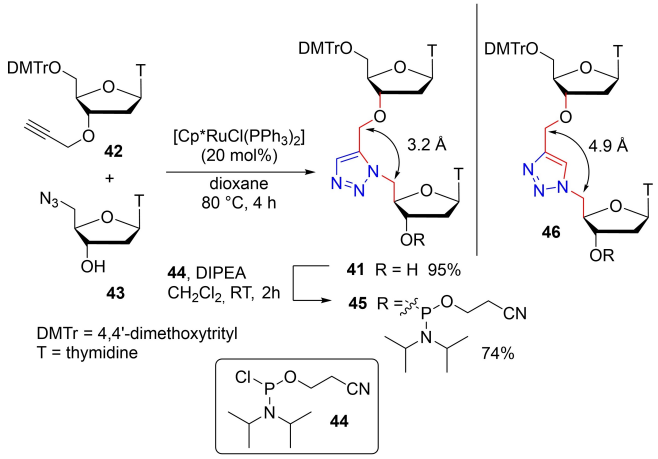

Scheme 20. Triazoles **45** and **46** as DNA phosphodiester backbone mimics

4.3. 1,5-Disubstituted 1,2,3-Triazoles with Anticancer Activity

The macrolactone migrastatin (Scheme 21) has been isolated from *Streptomyces platensis*, and together with several of its

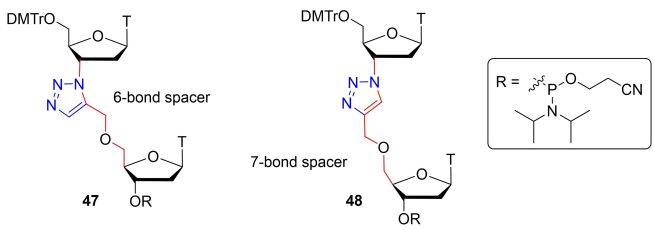

Figure 12. DNA backbone mimics **47** and **48** with 6- and 7-bond spacers.

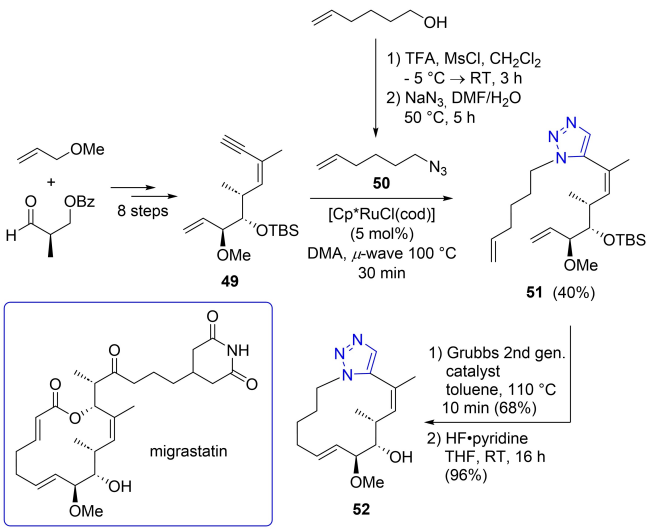

Scheme 21. Synthesis of a 1,5-disubstituted 1,2,3-triazole analogue (**52**) of the anticancer compound migrastatin.

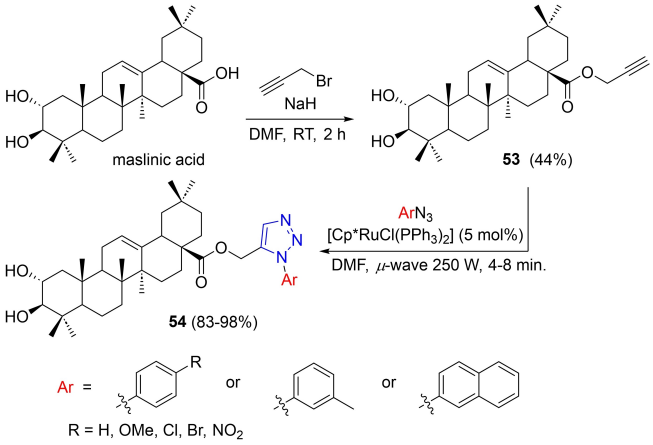

Scheme 22. Triazole derivatives (**54**) of maslinic acid.

analogues, shows promising anti-metastatic activity by targeting the actin-bundling activity of the protein facsin.[64] Murphy and Passarella have synthesized migrastatin analogues via CuAAC and RuAAC, replacing the lactone functionality of the original compound with a triazole and simplifying the structure by removing the side chain.[65] Alkyne **49** was first prepared in 8 steps from commercial starting materials, while azide **50** was synthesized in two steps from hex-5-enol via mesylation followed by nucleophilic displacement by azide ion. Compounds **49** and **50** were subsequently heated to 100 °C in DMA in the presence of 5 mol% [Cp*RuCl(cod)] under microwave conditions, forming triazole **51** in 40% yield. Ru-catalyzed metathesis was used to fuse the macrocycle and migrastatin analogue **52** was subsequently formed following TBS-deprotection under acidic conditions. Compound **52**, as well as its 1,4-disubstituted analogue, both showed promising capability in terms of inhibiting the migration of the human breast cancer cell line MDA-MB-361.

Maslinic acid (Scheme 22) is a pentacyclic triterpene found in olives, and displaying interesting biological activities, such as anti-inflammatory, anticancer and anti-HIV properties.[66] Ben Jannet and colleagues prepared triazole derivatives of maslinic acid in order to compare their anticancer activity and inflammatory activity with the original compound.[67] Maslinic acid itself was first converted to the propargylic ester **53** in 44% yield and subsequently reacted with a variety of aryl azides in the presence of 5 mol% [Cp*RuCl(PPh_3)$_2$] under microwave conditions. The desired triazole derivatives **54** were formed in high yields in a matter of minutes. The corresponding 1,4-disubstituted 1,2,3-triazole derivatives were also prepared using CuAAC. All prepared triazole derivatives showed more potent anti-inflammatory activity than maslinic acid itself. In terms of the anticancer activity of these derivatives, maslinic acid was found to be the most anti-proliferative against breast and colon cancer cell lines, while the triazole derivatives showed moderate to good activity, with the 1,4-disubstituted compounds possessing better activity than their 1,5-disubstitued isomeric counterparts **54**. The same group has also used RuAAC to prepare triazole derivatives of oleanolic acid, an analogue of maslinic acid, but lacking one hydroxy group.[68]

Naphthoquinones are common structures in anticancer drugs, examples being doxorubicin and mitoxantrone, both used clinically in cancer treatment.[69] da Silva Jr. and his group have earlier studied triazolyl naphthoquinones prepared via CuAAC,[70] and were interested in evaluating the antitumour potential of 1,5-disubstituted 1,2,3-triazolyl-lapachones **55**–**60** (Figure 13). The lapachones are a class of natural products originally isolated from the heartwood of *Tabebuia sp.*, also known as *ipe*, found in the American tropics and subtropics.[71] Triazoles **55**–**57** were prepared in a few steps from α-lapachone, nor-α-lapachone, and β-lapachone, respectively.[72] Triazole **58**, which is a derivative of nor-β-lapachone, was prepared from lapachol. An additional two naphtoquinones **59** and **60**, prepared from C-allyl lawsone, were also synthesized. [Cp*RuCl(PPh_3)$_2$] was used as the catalyst for the final RuAAC step, affording **55**–**60** in 30–60% yields. The antiparasitic

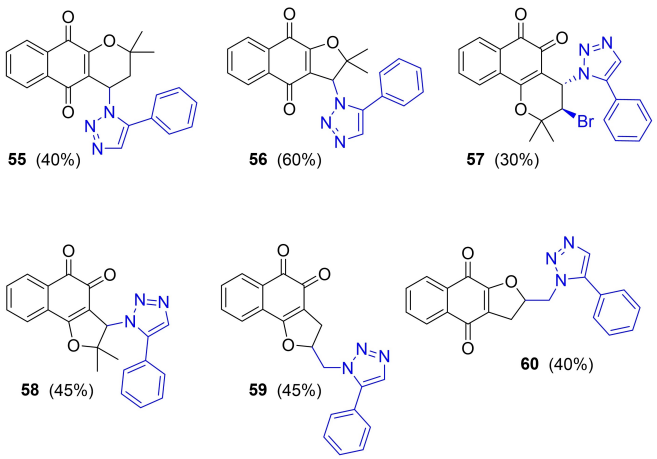

Figure 13. Naphthoquinone triazolyl derivatives **55**–**60** screened for antiparasitic and anticancer activity. Yields are for final RuAAC step in reaction sequence.

properties of these compounds against *T. cruzi*, which causes Chagas disease, was evaluated, where derivatives **57** and **58** showed activity in line with the standard treatment drug benznidazone. Screening **55**–**60** against several cancer cell lines showed compound **57** as a promising candidate, with better activity than doxorubicin for human prostate and melanoma cell lines, and also more active than its corresponding 1,4-disubstituted triazole isomer, making it a suitable candidate for further studies.

4.4. Compounds with Antibacterial and Antiparasitic Activity

Antibiotic-resistant bacteria are a major threat to human health and the situation is predicted to become worse in coming years.[73] The search for new antibacterial drugs is thus of utmost importance.[74] Triazole-containing compounds have shown promise in this context,[75] but studies on the use of 1,5-disubstituted 1,2,3-triazoles are limited.[76] Labadie and colleagues investigated the antitubercular activity of 1,2,3-triazole fatty acid derivatives, including both 1,4- and 1,5-disubstitued triazoles in their study.[77] The bond angles and distance between the substituents indicate that the 1,5-disubstituted triazole isomer can act as a mimic for a fatty acid *Z*-alkene. Compounds **61** were prepared from the corresponding alkyne and azide, using [Cp*RuCl(PPh$_3$)$_2$] as the catalyst (Scheme 23). The reaction was not completely regioselective, but the major 1,5-isomers **61** could be separated from the 1,4-isomers **62**. Compounds **61** were found to be substantially less active against the *M. tuberculosis* H37Rv strain than their 1,4-counterparts **62**, however.

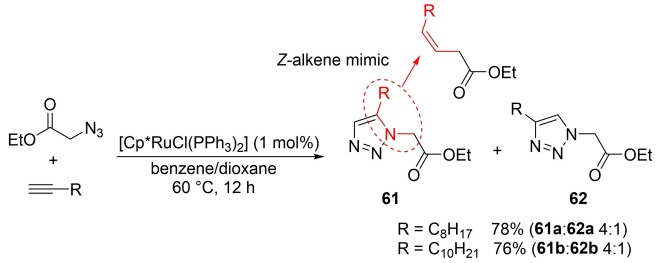

Scheme 23. Triazolyl fatty acid derivatives **61** and **62**, investigated for their potential antitubercular activity.

Triazole-substituted coumarine and quinolin-2(1H)-one derivatives **63** were synthesized by Anand and Kulkarni using 2 mol% [Cp*RuCl(PPh$_3$)$_2$] in dioxane (Scheme 24).[78] In addition to photophysical and crystallographical investigations of the prepared compounds, these derivatives were also screened for their antitubercular activity against *M. tuberculosis* H37Rv. All prepared compounds, including the corresponding 1,4-disubstituted 1,2,3-triazoles, displayed improved activity in comparison to commercial antibiotics such as streptomycin and ciprofloxacin. The lowest minimum inhibitory concentration (MIC) value, 0.4 μg/mL, was found for the 8-methyl quinolin-2(1H)-one derivative **63** (R = 8-Me, X=NH).

Antitubercular coumarine-triazole derivatives have been investigated by Lherbet and co-workers, who used click chemistry to couple diaryl ethers with coumarine fragments, mainly focusing on CuAAC but including also derivatives **64** prepared via RuAAC (Figure 14a).[79] However, in comparison to the 1,4-isomers, the 1,5-disubstituted triazole derivatives showed weaker inhibition of the targeted InhA enzyme. This enzyme is of importance in the biosynthesis of mycolic acid, a fatty acid found in the cell walls of *M. tuberculosis*, and InhA is thus a key target for new antitubercular drugs. Coumarine-triazole derivatives have also been reported by Tsogoeva and co-workers, but in this case RuAAC was used to prepare dimeric hybrids of the antimalarial drug artemisinine, using symmetrical internal alkynes as the substrates.[80] The prepared hybrids **65** showed excellent in vitro antimalarial activity against *P. falciparum* strains (Figure 14b).

Iannazzo has employed diazabicyclooctane (DBO) as a scaffold for preparing β-lactamase inhibitors **66** via RuAAC (Scheme 25).[81] Such compounds increase the efficacy when used in combination with an antibiotic. Reaction conditions for the preparation of **66** included 10 mol% [Cp*RuCl(cod)] as the catalyst, with DMF as the solvent, and heating the reaction for 24 hours at 70 °C. Five different 1,5-disubstituted 1,2,3-triazoles, as well as two 1,4,5-trisubstitued derivatives were prepared in 44–94% yield. The benzyloxy protecting group was subsequently exchanged for a sulfate functionality before screening derivatives **67** as β-lactamase KPC-2 inihibitors. The activity for these DBO compounds was found to be lower than commercial β-lactamase inhibitors, such as avibactam and relebactam, which is attributed to weaker hydrogen bonding interactions. However, molecular docking suggests that substitution on the

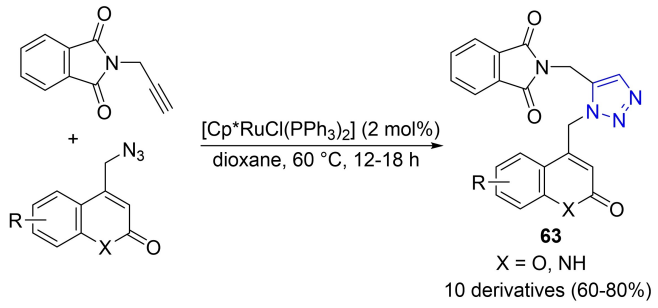

Scheme 24. Coumarine and quinolin-2(1H)-one triazole derivatives **63** with antitubercular activity.

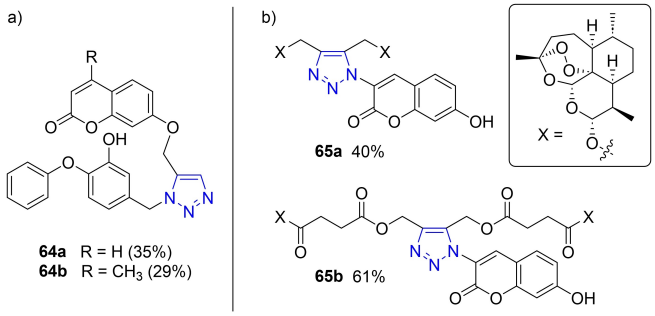

Figure 14. Coumarine-triazole derivatives in the preparation of antitubercular (**64**) and antimalarial (**65**) drugs.

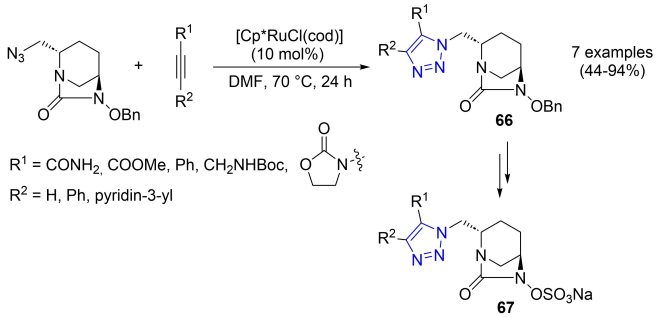

Scheme 25. Diazabicyclooctane-based triazole-containing β-lactamase inhibitors **67**.

triazole ring could afford further points of interaction and this could be a means to improve the activity of these DBO-based triazole derivatives.

Antibacterial compounds **68** (Scheme 26), based on a benzoxazine-2,4-dione scaffold, have been prepared by Kadri and colleagues using RuAAC. The derivatives showed moderate activity towards gram positive bacterial *S. aureus*, and *M. luteus* strains, as well as gram negative *P. aeruginosa* and *E. coli* strains.[82] The corresponding 1,4-disubstituted isomers were found to give more interesting results, however, with a few triazoles displaying improved activity compared to the standard drug tetracycline.

4.5. Carbohydrate Derivatives

While CuAAC has been extensively exploited in the field of glycoscience,[83] applications involving RuAAC are less frequent.[11] Koketsu and Kuberan prepared triazole-xylosides using RuAAC in order to investigate their capacity as primers in glycosaminoglycan biosynthesis.[84] Acetylated xylopyranoside azide, derived from D-xylose, was reacted with diynes of three different chain lengths to produce dimeric triazoles **69** (Scheme 27). Monomeric triazole derivatives **70** were also prepared, using aryl propargyl ethers as the alkyne components. Both **69** and **70** were found to have a higher priming ability than the corresponding 1,4-disubstited triazole derivatives. In addition, a shorter chain length (n = 1 or 2) was more beneficial than a longer chain length (n = 3). Computational

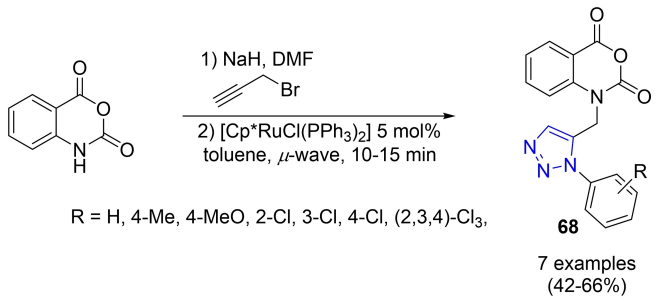

Scheme 26. Benzoxazine-2,4-dione-based triazole derivatives **68**.

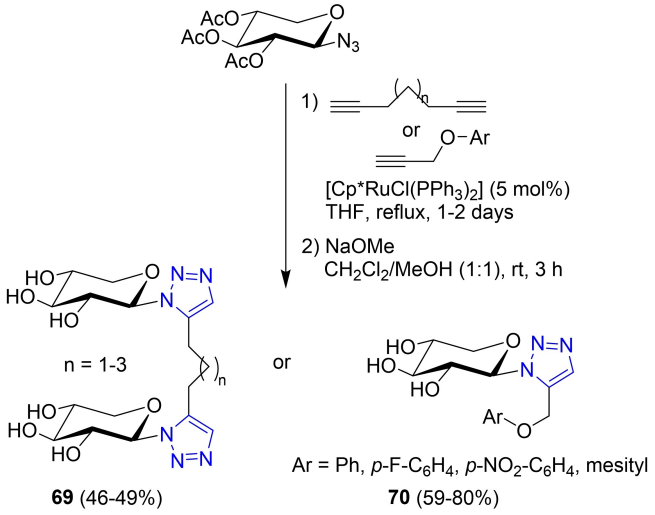

Scheme 27. Triazole-xyloside derivatives **69** and **70**, investigated as primers for glycosaminoglycan biosynthesis.

docking experiments were performed to clarify this behaviour, indicating that π-stacking interactions of these derivatives with tyrosine residues in β-1,4-galactosyltransferase 7, an enzyme of importance in glycosaminoglycan biosynthesis, could explain the higher priming activity.

Macrocyclization has already been mentioned in the context of peptidomimetics, but can also be applied towards other classes of biologically active molecules. The conformational preorganization achieved can enhance binding to a certain target and be beneficial for oral availability of pharmaceuticals and drug candidates.[85] van Calenbergh and co-workers prepared macrocyclic derivatives of the glycolipid α-galactosylceramide, of interest due to its immunomodulating properties (Scheme 28).[86] Azidoalkyne **71** was cyclized via RuAAC in 45% yield using [Cp*RuCl(cod)] as the catalyst, affording the glycosylated triazole **72** after benzyl deprotection. Biological evaluation showed that **72** did not possess the immunostimulating properties of the original α-galactosylceramide, however. The long lipid chains that form part of the original structure were not included in derivative **72** and this absence of

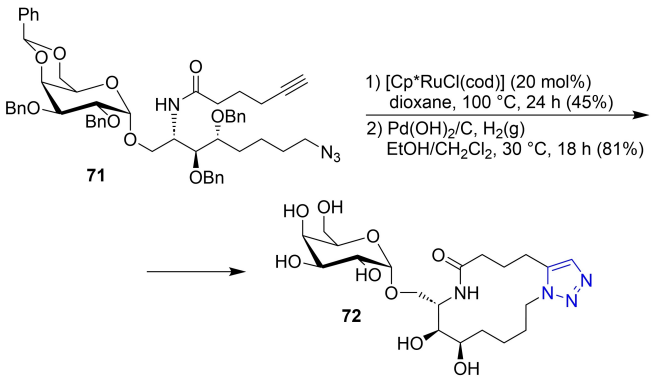

Scheme 28. Synthesis of macrocyclic α-galactosylceramide analogue **72**.

anchoring groups is postulated to be the reason behind the low activity.

The synthesis of migrastatin analogues using a combined RuAAC/metathesis approach has already been mentioned earlier (see Scheme 21).[65] Murphy and colleagues have also applied this strategy in diversity oriented synthesis, aiming to prepare macrocyclic scaffolds using building blocks from monosaccharides.[87] Scheme 29 shows the synthesis of one of these macrocycles (**73**), which could potentially be of interest as a galectin inhibitor. Microwave-mediated synthesis was used to couple azide **74** and alkyne **75**, forming a 1,5-disubstituted 1,2,3-triazole **76** in the process. Ruthenium-catalyzed metathesis was then used to close the ring, affording a 2:3 mixture of *cis* and *trans* isomers. The alkene isomers could be separated by flash chromatography, however, and removal of the protecting groups on the *trans* isomer produced the targeted macrocycle **73**.

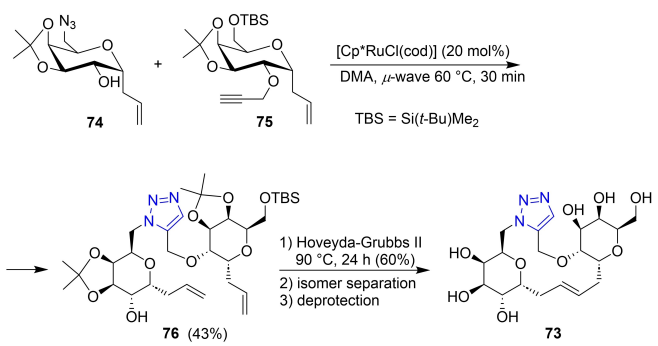

Scheme 29. Macrocycle formation using RuAAC and metathesis.

5. RuAAC in Polymer Synthesis

RuAAC has been applied in the synthesis of polymers using several different strategies, i.e. a) to prepare 1,5-disubstituted 1,2,3-triazole monomers for polymerization;[88] b) by performing the polymerization step itself via RuAAC;[89] c) for post-functionalization of a previously prepared polymer;[90] and d) to synthesize hyperbranched structures such as dendrimers.[91]

Triazole-containing monomers were prepared by Bizzarri and co-workers, aiming to apply these towards the preparation of luminescent metallopolymers, where a pyridyl-substituted triazole acts as a bidentate ligand for copper.[92] Such metallopolymers could potentially form components of organic light-emitting diodes. The monomers were prepared via a click reaction between homopropargylic alcohol **77** and benzyl azide, using [Cp*RuCl(cod)] as the catalyst, forming triazole **78** in 64% yield (Scheme 30). Compound **78** was subsequently equipped with two different polymerizable units, i.e. a styrene functionality and an acrylate group, to form monomers **79a** and **79b**. To investigate if copper complexation could be performed prior to polymerization, a second set of monomers, **80a** and **80b**, was also prepared by treating **79a** and **79b** with $Cu(MeCN)_4BF_4$ and DPEphos. Radical copolymerization of each monomer was then attempted in the presence of either styrene

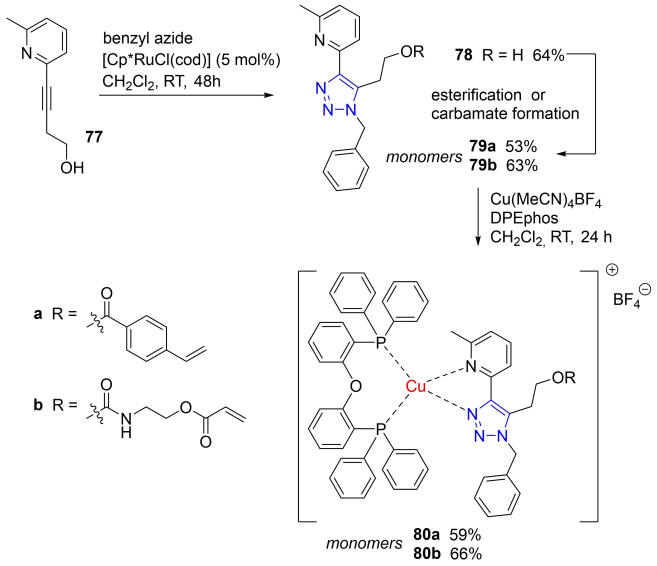

Scheme 30. Synthesis of monomers for luminescent metallopolymers **80** via RuAAC

(for **79a** and **80a**) or methyl acrylate (for **79b** and **80b**). Direct polymerization of the pre-prepared copper complexes **80a–b** was not successful; most likely the copper complex interferes with the radical polymerization. However, polymerization of monomers **79a** and **79b** afforded the corresponding copolymers, which could subsequently be functionalized with copper(I) to afford the targeted luminescent metallopolymers in good yields. The electrochemical and photophysical properties of both monomers **79** as well as the corresponding metallopolymers was subsequently investigated.

RuAAC can also be used for the polymerization step itself, and Hashidzume and co-workers employed this tactic in the synthesis of dense 1,2,3-triazole-containing oligomers prepared via RuAAC.[93] A model reaction was first performed, using azide **81** and alkyne **82** with 22 mol% $[Cp^*RuCl(PPh_3)_2]$ in THF, affording triazole **83** in 33% yield (Scheme 31). While all starting material was consumed, the low yield is attributed to dimerization of **82** as a side reaction, as well as the formation of some 1,4-disubstituted triazole. For the polymerization, azidoalkyne **84** was used as the monomer. Earlier studies showed that the regioselectivity could be improved using microwave heating instead of conventional heating, and these reactions were thus performed in a microwave reactor at 50 °C in THF for 8 hours. Using 20 mol% $[Cp^*RuCl(PPh_3)_2]$, the desired oligomer could be formed in 88% yield. ^1H NMR indicated that the molar fraction of the 1,5-disubstituted isomer was around 0.85, with some concomitant formation of the 1,4-disubstituted isomer, the latter attributed to steric hindrance in the formation of longer oligomers of the 1,5-isomer. The mass average molar mass M_W was determined for the polymer using size-exclusion chromatography (SEC) and was found to be around half the value of the corresponding polymer prepared via CuAAC. The RuAAC polymer was found to be soluble in most organic solvents, but not in water or hexanes.

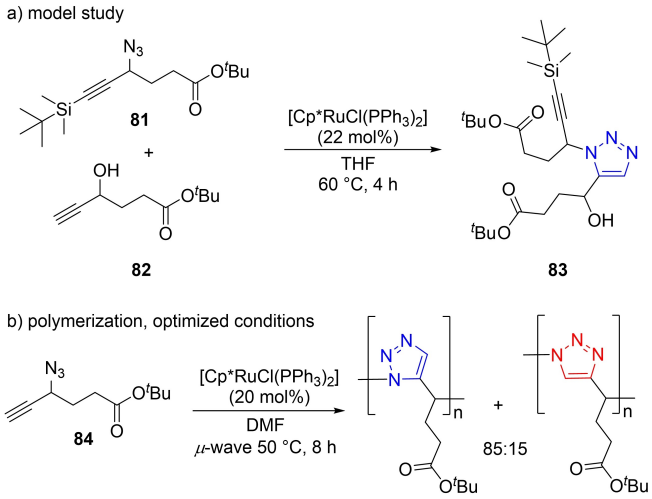

Scheme 31. Polymerization of monomer **84** using RuAAC.

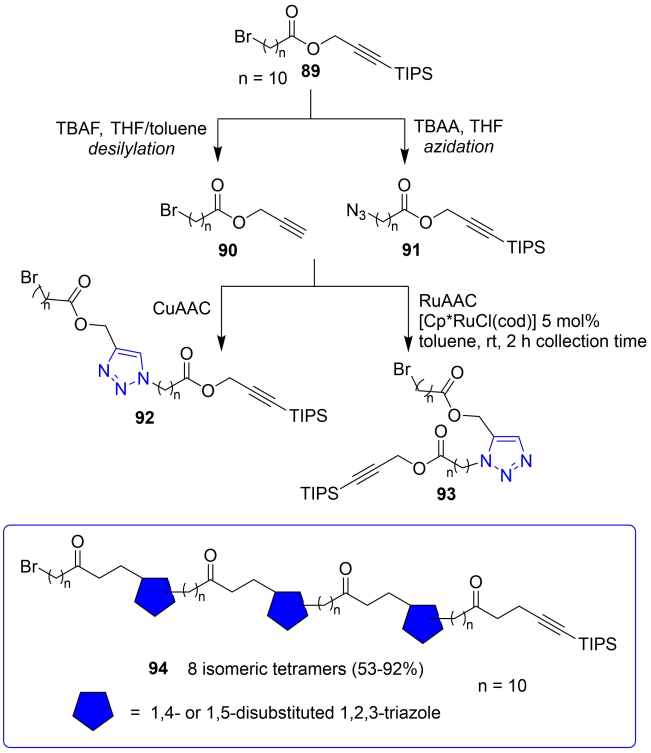

Scheme 33. Iterative flow synthesis of oligomers **94** with triazole linkages.

While CuAAC is normally employed for the synthesis of 1,4-disubstituted 1,2,3-triazoles, there may be situations where the use of a copper catalyst is not suitable. However, Ru-catalysts that lack the Cp* ligand can in some cases give high selectivity for the 1,4-disubstituted triazole isomer. Qin and Tang exploited this feature in developing a ligand-controlled regiodivergent RuAAC-type polymerization, where the presence or absence of a Cp* ligand on the ruthenium complex determines the regiochemical outcome.[94] Thus, reaction of dialkyne **85** and diazide **86** in the presence of $[RuH_2(CO)(PPh_3)_3]$ afforded polymer **87**, containing 1,4-disubstituted 1,2,3-triazole units (Scheme 32). Use of a ruthenium catalyst with a Cp* ligand produced the corresponding polymer **88**, but now with the 1,5-substitution pattern on the triazoles. The thermal, photophysical and optical properties of the two polymers were then compared, where both the glass temperature (T_g) as well as the refractive index was found to be higher for the 1,4-disubstituted isomer.

An iterative synthesis of triazole oligomers using flow chemistry has been reported by Jamison and colleagues.[95] They applied a method called iterative exponential growth (IEG), which allows the preparation of sequence-defined oligomers in a controlled fashion. Starting from the same monomeric precursor **89** (Scheme 33), which was either azidated or de-silylated in flow, and subsequently allowing the two resultant reagent streams of **90** and **91** to mix with a stream of either a copper catalyst solution or with 5 mol% [Cp*RuCl(cod)] in toluene, dimers **92** and **93** could be formed. By repeating the procedure, a set of eight tetramers **94**, with alternating 1,4- or 1,5-disubstituted 1,2,3-triazole linkages, were produced. The flow system could be scaled up to produce up to 2.75 g of material per hour.

In addition to incorporating triazoles into a polymer backbone, CuAAC and RuAAC can also be used for derivatizing cross-linkers for use in polymerization. Mikos and co-workers applied this strategy in the functionalization of hydrogels for applications in tissue engineering.[96] Many such hydrogels, as well as their corresponding synthetic cross-linkers, are bioinert and need to be modified in order to introduce tissue-specific chemical cues. A polyester cross-linker, with propargylic thiols at each end, was prepared and subsequently functionalized via RuAAC. Two different peptides (hydrophilic/hydrophobic) and one glycosaminoglycan, tagged with azide groups, were reacted with the polyester alkynes in the presence of 10 mol% [Cp*RuCl(cod)] in aqueous solution at ambient temperature, to afford three different tissue-specific biofunctionalized hydrogel cross-linkers **95** (Figure 15). The cross-linkers were incorporated into hydrogels, and the hydrolytic degradability, cytotoxicity and leachability of these new materials was subsequently assessed.

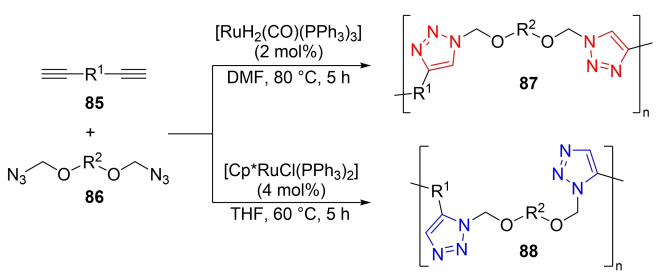

Scheme 32. Regiodivergent synthesis of triazole polymers **87** and **88** using ruthenium catalysts with and without a Cp* ligand.

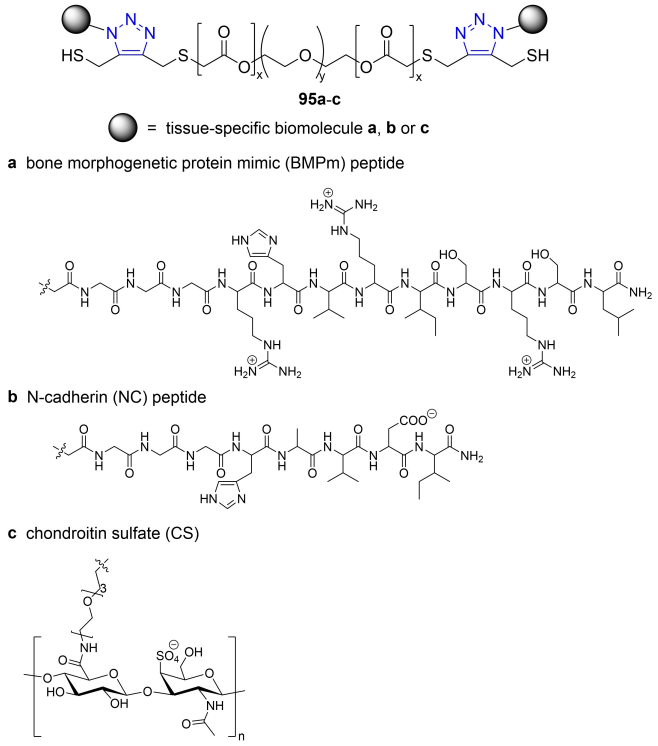

Figure 15. Tissue-specific biofunctionalized cross-linkers **95** for incorporation into hydrogels.

6. Physical Chemistry Applications

While the majority of applications involving RuAAC are found in medicinal chemistry and chemical biology, the aromatic nature of the triazole makes it well suited for incorporation into electronic devices, nanonsensors and molecular materials. Earlier examples include the use of 1,5-disubstituted or 1,4,5-trisubstitued triazoles in light-emitting diodes,[97] contrast agents for optoacoustic imaging,[98] fluorescent chemosensors,[99] dye-sensitized solar cells,[100] and non-linear optic materials.[101] One of the more recent examples in this context comes from Moth-Poulsen and co-workers, who investigated norbornadienes with triazole substituents as photoswitches, aiming to develop Molecular Solar Thermal Storage (MOST) systems.[102] The aim of the MOST device is to capture solar energy during the day and utilize it at night or at a later time. This process involves light-mediated conversion of the norbornadiene into a quadricyclane, where energy can be stored, followed by thermic cycloreversion to the original norbornadiene state, with concomitant heat release. The molecules in question belong to the T-type, i.e. while light is used for the original isomerization, they require heat for back-conversion. The optical absorbance of the photoswitch needs to overlap with the solar spectrum. The absorbance can be tailored using donor-acceptor substituents on one of the norbornadiene double bonds, and in this report, triazoles were investigated as potential acceptor groups. Norbornadienes **96** (Scheme 34), prepared via a Diels-Alder reaction with cyclopentadiene, were deprotected using potassium carbonate in

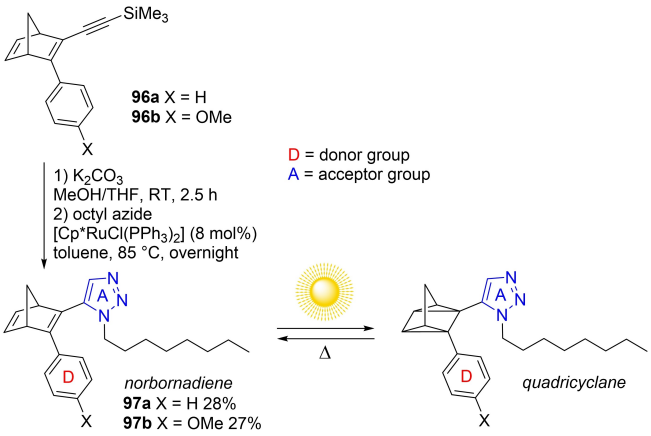

Scheme 34. Triazole-based photoswitches **97** for molecular energy storage.

methanol, and subsequently heated with octyl azide in the presence of $[Cp^*RuCl(PPh_3)_2]$ in toluene, affording the 1,5-disubstitued triazoles **97** in moderate yields. Compounds **97** were found to have long-lived quadricyclane states (220 days in the case of **97a**), which is beneficial for energy storage. However, the absorption onset as well as the quantum yields were found to be less attractive, indicating that further development work is required. The corresponding 1,4-disubstituted isomers were also prepared via CuAAC and displayed improved properties in comparison to the 1,5-isomers.

Diarylethenes (Scheme 35) have been extensively investigated for their photochromic properties, as photoirradiation effects a 6π-electrocyclization, which disrupts the aromatic pattern in the molecule and produces a colour change.[103] This property is useful for applications in molecular switches and optical memories. In contrast to compounds **97** described above, photochromic diarylethenes are classified as P-type, i.e. they are thermally irreversible but photochemically reversible. Yokoyama and co-workers have reported diarylethene analogues where the ethene backbone is replaced by a triazole and

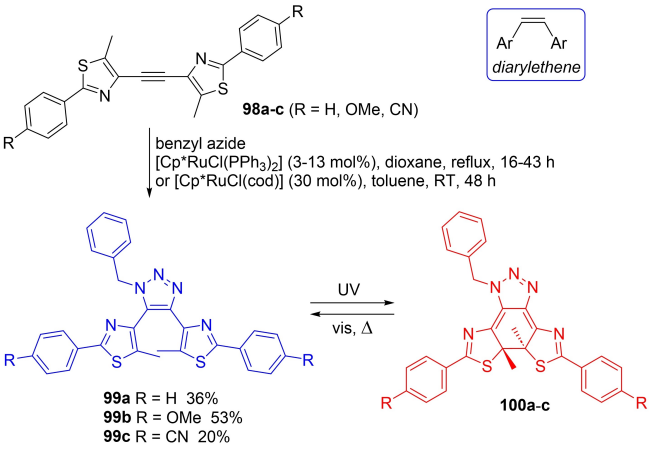

Scheme 35. Synthesis of reversible photochromic 4,5-bisthiazolyl-1,2,3-triazoles **100**.

studied their photochromic properties.[104] The precursor diarylethynes **98a-c** were assembled using Suzuki and Sonogashira reactions and subsequently cyclized to the corresponding triazoles **99a-c** via RuAAC. [Cp*RuCl(PPh$_3$)$_2$] was used as the catalyst for **99a** and **99c**, using dioxane as the solvent, while **99b** was formed using [Cp*RuCl(cod)] in toluene. The modest yields were ascribed to steric hindrance in the products. **99a-c** were irradiated in four different solvents using light with a wavelength of 313 nm. The thermal back-reaction was found to be faster for **100c** compared to **100a** and **100b**, which is ascribed to the electron-withdrawing properties of the cyano substituent. Absorption maxima for **100a–c** were in the range of 700–740 nm.

Karuso and colleagues employed a combinatorial approach for discovering new fluorophores via azide alkyne cycloaddition reactions, building on earlier studies by Fahrni[105] and Wang[106] that show that triazole formation can enhance the fluorescent properties of a compound.[107] A set of 20 azides and 11 alkynes, all non-fluorescent, were subjected to CuAAC conditions in a 96-well plate format, using $CuSO_4$ as the catalyst. A fluorescence plate reader was used to identify triazole fluorophores and the most interesting candidates were resynthesized on a larger scale in order to study their photophysical behaviour in more detail. For comparative purposes, the corresponding 1,5-isomer of **101a** was prepared via RuAAC, using 20 mol% [Cp*RuCl(PPh$_3$)$_2$] as the catalyst, forming **101b** in 83% yield (Figure 16). Interestingly, **101b** displayed a quantum yield that was nearly an order of magnitude larger than for **101a**. DFT calculations indicate that push-pull triazoles, with one electron deficient arene and one electron rich arene as substituents on the triazole, could be of interest for further studies in this context.

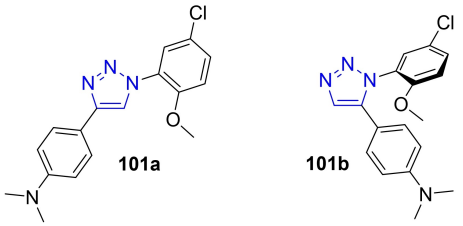

Figure 16. Fluorescent 1,4- and 1,5-triazole isomers **101a** and **101b**.

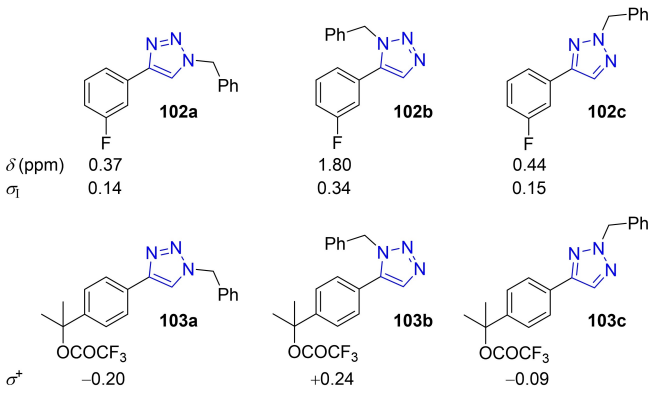

Figure 17. ^{1}H NMR chemical shifts and σ_I / $\sigma+$ values of compounds **102** and **103** for determining the inductive effects and cation-stabilizing ability of triazoles with different substitution patterns.

Creary et al have studied the photophysical properties of 1,2,3-triazoles with different substitution patterns and compared their ability to stabilize carbocations and radicals.[108] The inductive effect (σ_I) of a triazole group was first determined by ^{31}F NMR, using a method described by Taft, who observed that the σ_I value correlates with the ^{19}F NMR chemical shift in *meta*-substituted fluorobenzenes.[109] The chemical shifts and calculated σ_I values for triazoles **102** are shown in Figure 17, the results indicating that the 1,5-disubstituted triazole **102b** is significantly more electron-withdrawing than its isomeric structures **102a** and **102c**, with an inductive effect in line with an acetyl group. Triazole **102b** was prepared in 89% yield, by refluxing benzyl azide and 1-ethynyl-3-fluorobenzene in benzene for 5 hours, using 2 mol% [Cp*RuCl(PPh$_3$)$_2$] as the catalyst. The ability to stabilize a cationic charge (σ^+) was subsequently investigated using *para*-triazolyl substituted benzylic trifluoroacetates **103** and comparing their rate of solvolysis. While **103a** and **103c** were found to react faster than cumyl trifluoroacetate, which lacks a triazole substituent, **103b** instead has a slower rate of acetolysis, further confirming the electron-withdrawing nature of the 1,5-disubstituted triazole. The same group has also reported a useful method for differentiation between 1,4- and 1,5-disubstituted 1,2,3-triazole isomers using one-dimensional ^{13}C NMR with gated decoupling.[110]

7. Summary and Outlook

While less known that its copper-catalyzed counterpart, the ruthenium-catalyzed azide alkyne cycloaddition (RuAAC) has rapidly gained the interest of the research community, with applications in a wide range of areas. Examples include the synthesis of compounds with potential anticancer, antibacterial and antimalarial activity, as well as for derivatizing peptidomimetics. Other fields where this reaction has been applied are in the synthesis of functionalized polymers, photoswitches and photochromic devices. RuAAC not only allows the selective formation of 1,5-disubstituted 1,2,3-triazoles, but is also compatible with internal alkynes, thus providing access to 1,4,5-trisubstituted triazoles. A current limitation, however, is that the regiochemical outcome is strongly dependent on the structure of the internal alkyne, meaning that not all substitution patterns are accessible. Further catalyst development in this field could potentially be one way to address this problem. We envisage many new and exciting developments and applications of this reaction in coming years.

Acknowledgements

This project has received funding from the European Union's Horizon 2020 research and innovation programme under the Marie Skłodowska-Curie grant agreement No. 955626 (FF and NK). Financial support from the Nano Area of Advance at

Chalmers is gratefully acknowledged (NK), as are grants from the Ministry of Innovation and Technology of Hungary, from the National Research, Development and Innovation Fund, TKP2021-EGA-31, KKP22 144180, and the 2020–1-1-2-PIACI-KFI_2020-00021 funding schemes (TBS).

Conflict of Interests

The authors declare no conflict of interest.

Data Availability Statement

Data sharing is not applicable to this article as no new data were created or analyzed in this study.

Keywords: ruthenium · transition-metal catalysis · cycloaddition · triazole · alkyne

[1] H. C. Kolb, M. G. Finn, K. B. Sharpless, *Angew. Chem. Int. Ed.* **2001**, *40*, 2004–2021.
[2] a) A. Michael, *J. Prakt. Chem.* **1893**, *48*, 94–95; b) R. Huisgen, *Angew. Chem.* **1963**, *75*, 604–637; c) R. Huisgen, *Angew. Chem.* **1963**, *75*, 742–745.
[3] C. L. Wang, D. Ikhlef, S. Kahlal, J. Y. Saillard, D. Astruc, *Coord. Chem. Rev.* **2016**, *316*, 1–20.
[4] a) R. Huisgen, in *1,3-Dipolar Cycloaddition Chemistry, Vol. 1* (Ed.: A. Padwa), Wiley Interscience, New York, **1984**, pp. 1–176; b) S. E. Beutick, P. Vermeeren, T. A. Hamlin, *Chem. Asian J.* **2022**, *17*, e202200553.
[5] C. W. Tornoe, C. Christensen, M. Meldal, *J. Org. Chem.* **2002**, *67*, 3057–3064.
[6] V. V. Rostovtsev, L. G. Green, V. V. Fokin, K. B. Sharpless, *Angew. Chem. Int. Ed.* **2002**, *41*, 2596–2599.
[7] a) G. Akimova, V. Chistokletov, A. Petrov, *Zh. Obshch. Khim.* **1967**, *3*, 968–974; b) A. Krasinski, V. V. Fokin, K. B. Sharpless, *Org. Lett.* **2004**, *6*, 1237–1240.
[8] L. Zhang, X. G. Chen, P. Xue, H. H. Y. Sun, I. D. Williams, K. B. Sharpless, V. V. Fokin, G. C. Jia, *J. Am. Chem. Soc.* **2005**, *127*, 15998–15999.
[9] Y. Yamamoto, T. Arakawa, R. Ogawa, K. Itoh, *J. Am. Chem. Soc.* **2003**, *125*, 12143–12160.
[10] J. H. Ma, S. T. Ding, *Asian J. Org. Chem.* **2020**, *9*, 1872–1888.
[11] J. R. Johansson, T. Beke-Somfai, A. S. Stålsmeden, N. Kann, *Chem. Rev.* **2016**, *116*, 14726–14768.
[12] B. C. Boren, S. Narayan, L. K. Rasmussen, L. Zhang, H. T. Zhao, Z. Y. Lin, G. C. Jia, V. V. Fokin, *J. Am. Chem. Soc.* **2008**, *130*, 8923–8930.
[13] M. Ahlquist, V. V. Fokin, *Organometallics* **2007**, *26*, 4389–4391.
[14] M. M. Majireck, S. M. Weinreb, *J. Org. Chem.* **2006**, *71*, 8680–8683.
[15] Y. Yousfi, W. Benchouk, S. M. Mekelleche, *Theor. Chem. Acc.* **2021**, *140*, 4.
[16] a) F. Himo, T. Lovell, R. Hilgraf, V. V. Rostovtsev, L. Noodleman, K. B. Sharpless, V. V. Fokin, *J. Am. Chem. Soc.* **2005**, *127*, 210–216; b) E. Boz, N. S. Tüzün, *J. Organomet. Chem.* **2013**, *724*, 167–176.
[17] Y. Yousfi, W. Benchouk, S. M. Mekelleche, *Chem. Heterocycl. Compd.* **2023**, 118–127.
[18] R. F. W. Bader, H. Essén, *J. Chem. Phys.* **1984**, *80*, 1943–1960.
[19] T. Hosseinnejad, S. Mandavian, *Comput. Theor. Chem.* **2018**, *1143*, 29–35.
[20] M. H. Baghersad, A. Habibi, A. D. Nejad, *RSC Adv.* **2023**, *13*, 28527–28541.
[21] A. K. Malde, L. Zuo, M. Breeze, M. Stroet, D. Poger, P. C. Nair, C. Oostenbrink, A. E. Mark, *J. Chem. Theory Comput.* **2011**, *7*, 4026–4037.
[22] P. N. Liu, H. X. Siyang, L. Zhang, S. K. S. Tse, G. C. Jia, *J. Org. Chem.* **2012**, *77*, 5844–5849.
[23] T. Keicher, S. Löbbecke, in *Organic Azides: Synthesis and Applications* (Eds.: S. Bräse, K. Banert), John Wiley and Sons, Ltd, Chichester, **2010**, pp. 1–27.
[24] S. Oppilliart, G. Mousseau, L. Zhang, G. C. Jia, P. Thuery, B. Rousseau, J. C. Cintrat, *Tetrahedron* **2007**, *63*, 8094–8098.
[25] S. Ramasamy, C. Petha, S. Tendulkar, P. Maity, M. D. Eastgate, R. Vaidyanathan, *Org. Process Res. Dev.* **2018**, *22*, 880–887.
[26] R. Jamatia, A. Gupta, M. Mahato, R. A. Patil, Y. R. Ma, A. K. Pal, *ChemistrySelect* **2016**, *1*, 5929–5935.
[27] Y. M. A. Yamada, S. M. Sarkar, Y. Uozumi, *J. Am. Chem. Soc.* **2012**, *134*, 9285–9290.
[28] A. Gupta, R. Jamatia, M. Mahato, A. K. Pal, *Ind. Eng. Chem. Res.* **2017**, *56*, 2375–2382.
[29] P. Sharma, J. Rathod, A. P. Singh, P. Kumar, Y. Sasson, *Catal. Sci. Technol.* **2018**, *8*, 3246–3259.
[30] W. A. A. Arafa, A. A. Nayl, *Appl. Organomet. Chem.* **2019**, *33*, e5156.
[31] P. C. Knutson, H. E. Fredericks, E. M. Ferreira, *Org. Lett.* **2018**, *20*, 6845–6849.
[32] S. Yoshida, K. Kanno, I. Kii, Y. Misawa, M. Hagiwara, T. Hosoya, *Chem. Commun.* **2018**, *54*, 3705–3708.
[33] S. Yoshida, Y. Sakata, Y. Misawa, T. Morita, T. Kuribara, H. Ito, Y. Koike, I. Kii, T. Hosoya, *Chem. Commun.* **2021**, *57*, 899–902.
[34] P. Destito, J. R. Couceiro, H. Faustino, F. Lopez, J. L. Mascarenas, *Angew. Chem. Int. Ed.* **2017**, *56*, 10766–10770.
[35] A. Gutierrez-Gonzalez, P. Destito, J. R. Couceiro, C. Perez-Gonzalez, F. Lopez, J. L. Mascarenas, *Angew. Chem. Int. Ed.* **2021**, *60*, 16059–16066.
[36] B. T. Worrell, J. A. Malik, V. V. Fokin, *Science* **2013**, *340*, 457–460.
[37] W. Z. Song, M. Li, K. Dong, Y. B. Zheng, *Adv. Synth. Catal.* **2019**, *361*, 5258–5263.
[38] D. Bhatt, P. R. Singh, P. Kalaramna, K. Kumar, A. Goswami, *Adv. Synth. Catal.* **2019**, *361*, 5483–5489.
[39] E. Engholm, N. Stuhr-Hansen, O. Blixt, *Tetrahedron Lett.* **2017**, *58*, 2272–2275.
[40] a) K. Bozorov, J. Y. Zhao, H. A. Aisa, *Bioorg. Med. Chem.* **2019**, *27*, 3511–3531; b) X. Y. Jiang, X. Hao, L. L. Jing, G. C. Wu, D. W. Kang, X. Y. Liu, P. Zhan, *Expert Opin. Drug Discovery* **2019**, *14*, 779–789.
[41] D. S. Pedersen, A. Abell, *Eur. J. Org. Chem.* **2011**, 2399–2411.
[42] H. Minnee, H. Chung, J. G. M. Rack, G. A. van der Marel, H. S. Overkleeft, J. D. C. Codee, I. Ahel, D. V. Filippov, *J. Org. Chem.* **2023**, *88*, 10801–10809.
[43] P. Mucha, M. Pieszko, A. Miszka, J. Ruczynski, P. Rekowski, I. Zaluska, A. Kozlowska, A. Schumacher, M. Deptula, M. Pikula, *Lett. Org. Chem.* **2018**, *15*, 282–289.
[44] X. Z. Zhao, K. Tsuji, D. Hymel, T. R. Burke, *Molecules* **2019**, *24*, 1488.
[45] N. G. Angelo, P. S. Arora, *J. Am. Chem. Soc.* **2005**, *127*, 17134–17135.
[46] a) J. R. Johansson, E. Hermansson, B. Nordén, N. Kann, T. Beke-Somfai, *Eur. J. Org. Chem.* **2014**, *2014*, 2703–2713; b) N. Kann, J. R. Johansson, T. Beke-Somfai, *Org. Biomol. Chem.* **2015**, *13*, 2776–2785.
[47] A. S. Stålsmeden, A. J. Paterson, I. C. Szigyarto, L. Thunberg, J. R. Johansson, T. Beke-Somfai, N. Kann, *Org. Biomol. Chem.* **2020**, *18*, 1957–1967.
[48] O. Kracker, J. Gora, J. Krzciuk-Gula, A. Marion, B. Neumann, H. G. Stammler, A. Niess, I. Antes, R. Latajka, N. Sewald, *Chem. Eur. J.* **2018**, *24*, 953–961.
[49] J. A. Ellman, *Pure Appl. Chem.* **2003**, *75*, 39–46.
[50] a) J. Q. Zhang, J. Kemmink, D. T. S. Rijkers, R. M. J. Liskamp, *Org. Lett.* **2011**, *13*, 3438–3441; b) J. Zhang, J. Kemmink, D. T. S. Rijkers, R. M. J. Liskamp, *Biopolymers* **2011**, *96*, 444–444.
[51] J. Q. Zhang, J. Kemmink, D. T. S. Rijkers, R. M. J. Liskamp, *Chem. Commun.* **2013**, *49*, 4498–4500.
[52] X. Yang, L. P. Beroske, J. Kemmink, D. T. S. Rijkers, R. M. J. Liskamp, *Tetrahedron Lett.* **2017**, *58*, 4542–4546.
[53] X. Yang, J. Kemmink, D. T. S. Rijkers, R. M. J. Liskamp, *Bioorg. Med. Chem. Lett.* **2022**, *73*, 128887.
[54] A. Gori, P. Gagni, S. Rinaldi, *Chem. Eur. J.* **2017**, *23*, 14987–14995.
[55] S. Pacifico, A. Kerckhoffs, A. J. Fallow, R. E. Foreman, R. Guerrini, J. McDonald, D. G. Lambert, A. G. Jamieson, *Org. Biomol. Chem.* **2017**, *15*, 4704–4710.
[56] S. Flohr, M. Kurz, E. Kostenis, A. Brkovich, A. Fournier, T. Klabunde, *J. Med. Chem.* **2002**, *45*, 1799–1805.
[57] L. W. Guddat, J. L. Martin, L. Shan, A. B. Edmundson, W. R. Gray, *Biochemistry* **1996**, *35*, 11329–11335.
[58] A. Knuhtsen, C. Whitmore, F. S. McWhinnie, L. McDougall, R. Whiting, B. O. Smith, C. M. Timperley, A. C. Green, K. I. Kinnear, A. G. Jamieson, *Chem. Sci.* **2019**, *10*, 1671–1676.
[59] S. R. Tala, A. Singh, C. J. Lensing, S. M. Schnell, K. T. Freeman, J. R. Rocca, C. Haskell-Luevano, *ACS Chem. Neurosci.* **2018**, *9*, 1001–1013.

[60] A. M. White, S. J. de Veer, G. J. Wu, P. J. Harvey, K. Yap, G. J. King, J. E. Swedberg, C. N. K. Wang, R. H. P. Law, T. Durek, D. J. Craik, *Angew. Chem. Int. Ed.* **2020**, *59*, 11273–11277.
[61] A. H. El-Sagheer, T. Brown, *Chem. Sci.* **2014**, *5*, 253–259.
[62] a) A. H. El-Sagheer, T. Brown, *Chem. Soc. Rev.* **2010**, *39*, 1388–1405; b) A. H. El-Sagheer, T. Brown, *Acc. Chem. Res.* **2012**, *45*, 1258–1267.
[63] a) Y. R. Baker, D. Traore, P. Wanat, A. Tyburn, A. H. El-Sagheer, T. Brown, *Tetrahedron* **2020**, *76*; b) S. Epple, A. Modi, Y. R. Baker, E. Wegrzyn, D. Traore, P. Wanat, A. E. S. Tyburn, A. Shivalingam, L. Taemaitree, A. H. El-Sagheer, T. Brown, *J. Am. Chem. Soc.* **2021**, *143*, 16293–16301.
[64] L. Chen, S. Y. Yang, J. Jakoncic, J. J. Zhang, X. Y. Huang, *Nature* **2010**, *464*, 1062–1066.
[65] A. Gabba, S. Robakiewicz, B. Taciak, K. Ulewicz, G. Broggini, G. Rastelli, M. Krol, P. V. Murphy, D. Passarella, *Eur. J. Org. Chem.* **2017**, *2017*, 60–69.
[66] Z. Jing, W. Rui, L. Ruihua, Y. Hao, F. Hengtong, *Curr. Drug Targets* **2021**, *22*, 1496–1506.
[67] K. Chouaib, S. Delemasure, P. Dutartre, H. Ben Jannet, *J. Enzyme Inhib. Med. Chem.* **2016**, *31*, 130–147.
[68] K. Chouaib, A. Romdhane, S. Delemasure, P. Dutartre, N. Elie, D. Touboul, H. Ben Jannet, *Arab. J. Chem.* **2019**, *12*, 3732–3742.
[69] C. E. Pereyra, R. F. Dantas, S. B. Ferreira, L. P. Gomes, F. P. Silva, *Cancer Cell Int.* **2019**, *19*, 207.
[70] a) E. N. da Silva, B. C. Cavalcanti, T. T. Guimaraes, M. Pinto, I. O. Cabral, C. Pessoa, L. V. Costa-Lotufo, M. O. de Moraes, C. K. Z. de Andrade, M. R. dos Santos, C. A. de Simone, M. O. F. Goulart, A. V. Pinto, *Eur. J. Med. Chem.* **2011**, *46*, 399–410; b) E. H. G. Da Cruz, C. M. B. Hussene, G. G. Dias, E. B. T. Diogo, I. M. M. De Melo, B. L. Rodrigues, M. G. Da Silva, W. O. Valenca, C. A. Camara, R. N. de Oliveira, Y. G. de Paiva, M. O. F. Goulart, B. C. Cavalcanti, C. Pessoa, E. N. Da Silva, *Bioorg. Med. Chem.* **2014**, *22*, 1608–1619; c) G. A. M. Jardim, W. J. Reis, M. F. Ribeiro, F. M. Ottoni, R. J. Alves, T. L. Silva, M. O. F. Goulart, A. L. Braga, R. F. S. Menna-Barreto, K. Salomao, S. L. De Castroe, E. N. Da Silva, *RSC Adv.* **2015**, *5*, 78047–78060.
[71] E. N. da Silva, G. A. M. Jardim, C. Jacob, U. Dhawa, L. Ackermann, S. L. De Castro, *Eur. J. Med. Chem.* **2019**, *179*, 863–915.
[72] S. B. B. B. Bahia, W. J. Reis, G. A. M. Jardim, F. T. Souto, C. A. de Simone, C. C. Gatto, R. F. S. Menna-Barreto, S. L. de Castro, B. C. Cavalcanti, C. Pessoa, M. H. Araujoa, E. F. da Silva Jr., *MedChemComm* **2016**, *7*, 1555–1563.
[73] Global Antimicrobial Resistance and Use Surveillance System (GLASS) report 2022. Geneva: World Health Organization; 2022.
[74] M. Miethke, M. Pieroni, T. Weber, M. Bronstrup, P. Hammann, L. Halby, P. B. Arimondo, P. Glaser, B. Aigle, H. B. Bode, R. Moreira, Y. N. Li, A. Luzhetskyy, M. H. Medema, J. L. Pernodet, M. Stadler, J. R. Tormo, O. Genilloud, A. W. Truman, K. J. Weissman, E. Takano, S. Sabatini, E. Stegmann, H. Brotz-Oesterhelt, W. Wohlleben, M. Seemann, M. Empting, A. K. H. Hirsch, B. Loretz, C. M. Lehr, A. Titz, J. Herrmann, T. Jaeger, S. Alt, T. Hesterkamp, M. Winterhalter, A. Schiefer, K. Pfarr, A. Hoerauf, H. Graz, M. Graz, M. Lindvall, S. Ramurthy, A. Karlen, M. van Dongen, H. Petkovic, A. Keller, F. Peyrane, S. Donadio, L. Fraisse, L. J. V. Piddock, I. H. Gilbert, H. E. Moser, R. Muller, *Nat. Chem. Rev.* **2021**, *5*, 726–749.
[75] B. Zhang, *Eur. J. Med. Chem.* **2019**, *168*, 357–372.
[76] M. R. Hansen, T. H. Jakobsen, C. G. Bang, A. E. Cohrt, C. L. Hansen, J. W. Clausen, S. T. Le Quement, T. Tolker-Nielsen, M. Givskov, T. E. Nielsen, *Bioorg. Med. Chem.* **2015**, *23*, 1638–1650.
[77] D. G. Ghiano, A. De la Iglesia, N. N. Liu, P. J. Tonge, H. R. Morbidoni, G. R. Labadie, *Eur. J. Med. Chem.* **2017**, *125*, 842–852.
[78] A. Anand, M. V. Kulkarni, *Synth. Commun.* **2017**, *47*, 722–733.
[79] M. Chebaiki, E. Delfourne, R. Tamhaev, S. Danoun, F. Rodriguez, P. Hoffmann, E. Grosjean, F. Goncalves, J. Azéma-Despeyroux, A. Pál, J. Korduláková, N. Preuilh, S. Britton, P. Constant, H. Marrakchi, L. Maveyraud, L. Mourey, C. Lherbet, *Eur. J. Med. Chem.* **2023**, *259*, 115646.
[80] L. Herrmann, M. Leidenberger, A. S. de Morais, C. Mai, A. Çapci, M. D. B. Silva, F. Plass, A. Kahnt, D. R. M. Moreira, B. Kappes, S. B. Tsogoeva, *Chem. Sci.* **2023**, *14*, 12941–12952.
[81] F. Bouchet, J. P. Barnier, I. Sayah, Y. Bagdad, M. A. Miteva, M. Arthur, M. Etheve-Quelquejeu, L. Iannazzo, *ChemMedChem* **2023**, *18*, e202300077.
[82] M. Ben Hammouda, I. Ahmad, A. Hamdi, A. Dbeibia, H. Patel, N. Bouali, W. S. Hamadou, K. Hosni, S. Ghannay, F. Alminderej, E. Noumi, M. Snoussi, K. Aouadi, A. Kadri, *Arab. J. Chem.* **2022**, *15*, 104226.
[83] A. K. Agrahari, P. Bose, M. K. Jaiswal, S. Rajkhowa, A. S. Singh, S. Hotha, N. Mishra, V. K. Tiwari, *Chem. Rev.* **2021**, *121*, 7638–7955.
[84] C. P. Mencio, D. R. Garud, Y. Doi, Y. L. Bi, H. Vankayalapati, M. Koketsu, B. Kuberan, *Bioorg. Med. Chem. Lett.* **2017**, *27*, 5027–5030.
[85] F. Giordanetto, J. Kihlberg, *J. Med. Chem.* **2014**, *57*, 278–295.
[86] J. Janssens, J. Van der Eycken, S. Van Calenbergh, *Eur. J. Org. Chem.* **2019**, *2019*, 2253–2267.
[87] K. A. Fox, R. Chadda, F. Cardona, S. Barron, P. McArdle, P. V. Murphy, *Tetrahedron* **2020**, *76*, 131495.
[88] a) H. Nulwala, K. Takizawa, A. Odukale, A. Khan, R. J. Thibault, B. R. Taft, B. H. Lipshutz, C. J. Hawker, *Macromolecules* **2009**, *42*, 6068–6074; b) A. Praud, O. Bootzeek, Y. Blache, *Green Chem.* **2013**, *15*, 1138–1141.
[89] a) M. R. Brei, R. H. Cooke III, D. J. Hanson, C. T. Gray, R. F. Storey, *J. Macromol. Sci. A* **2016**, *53*, 413–423; b) S. E. Brady, G. V. Shultz, D. R. Tyler, *J. Inorg. Organomet. Polym. Mater.* **2010**, *20*, 511–518.
[90] a) J. S. Oakdale, R. K. Sit, V. V. Fokin, *Chem. Eur. J.* **2014**, *20*, 11101–11110; b) R. Pola, A. Braunova, R. Laga, M. Pechar, K. Ulbrich, *Polym. Chem.* **2014**, *5*, 1340–1350.
[91] a) A. J. Qin, J. W. Y. Lam, C. K. W. Jim, L. Zhang, J. J. Yan, M. Haussler, J. Z. Liu, Y. Q. Dong, D. H. Liang, E. Q. Chen, G. C. Jia, B. Z. Tang, *Macromolecules* **2008**, *41*, 3808–3822; b) S. E. Brady, D. R. Tyler, *J. Inorg. Organomet. Polym. Mater.* **2013**, *23*, 158–166.
[92] F. Ferrari, J. Braun, C. E. Anson, B. D. Wilts, D. Moatsou, C. Bizzarri, *Molecules* **2021**, *26*, 2567.
[93] R. Taguchi, M. Nakahata, Y. Kamon, A. Hashidzume, *Polymer* **2023**, *15*, 2199.
[94] D. Huang, Y. Liu, A. J. Qin, B. Z. Tang, *Macromolecules* **2019**, *52*, 1985–1992.
[95] A. C. Wicker, F. A. Leibfarth, T. F. Jamison, *Polym. Chem.* **2017**, *8*, 5786–5794.
[96] J. L. Guo, Y. S. Kim, V. Y. Xie, B. T. Smith, E. Watson, J. Lam, H. A. Pearce, P. S. Engel, A. G. Mikos, *Sci. Adv.* **2019**, *5*, eaaw7396.
[97] E. Orselli, R. Q. Albuquerque, P. M. Fransen, R. Frohlich, H. M. Janssen, L. De Cola, *J. Mater. Chem.* **2008**, *18*, 4579–4590.
[98] E. Locatelli, G. Ori, M. Fournelle, R. Lemor, M. Montorsi, M. C. Franchini, *Chem. Eur. J.* **2011**, *17*, 9052–9056.
[99] Y. B. Ruan, Y. H. Yu, C. Li, N. Bogliotti, J. Tang, J. Xie, *Tetrahedron* **2013**, *69*, 4603–4608.
[100] S. Sinn, B. Schulze, C. Friebe, D. G. Brown, M. Jager, E. Altuntas, J. Kubel, O. Guntner, C. P. Berlinguette, B. Dietzek, U. S. Schubert, *Inorg. Chem.* **2014**, *53*, 2083–2095.
[101] D. Lumpi, F. Glocklhofer, B. Holzer, B. Stoger, C. Hametner, G. A. Reider, J. Frohlich, *Cryst. Growth Des.* **2014**, *14*, 1018–1031.
[102] A. U. Petersen, M. Jevric, K. Moth-Poulsen, *Eur. J. Org. Chem.* **2018**, *2018*, 4465–4474.
[103] M. Irie, T. Fulcaminato, K. Matsuda, S. Kobatake, *Chem. Rev.* **2014**, *114*, 12174–12277.
[104] C. X. Zhang, K. Morinaka, M. Kose, T. Ubukata, Y. Yokoyama, *Beilstein J. Org. Chem.* **2019**, *15*, 2161–2169.
[105] Z. Zhou, C. J. Fahrni, *J. Am. Chem. Soc.* **2004**, *126*, 8862–8863.
[106] K. Sivakumar, F. Xie, B. M. Cash, S. Long, H. N. Barnhill, Q. Wang, *Org. Lett.* **2004**, *6*, 4603–4606.
[107] F. Cleemann, W. L. Kum-Cheung, P. Karuso, *Tetrahedron Lett.* **2022**, *88*, 153520.
[108] X. Creary, K. Chormanski, G. Peirats, C. Renneburg, *J. Org. Chem.* **2017**, *82*, 5720–5730.
[109] R. W. Taft, I. C. Lewis, E. Price, K. K. Andersen, I. R. Fox, G. T. Davis, *J. Am. Chem. Soc.* **1963**, *85*, 709–724.
[110] X. Creary, A. Anderson, C. Brophy, F. Crowell, Z. Funk, *J. Org. Chem.* **2012**, *77*, 8756–8761.

Manuscript received: January 29, 2024
Revised manuscript received: May 6, 2024
Accepted manuscript online: May 10, 2024
Version of record online: June 18, 2024